Article

Not peer-reviewed version

Development of New Resolvin D1 Analogues for Osteoarthritis Therapy: Acellular and Computational Approaches to Study Their Antioxidant Activities

Zahra Kariminezhad , Mahdi Rahimi , Julio Fernandes , Donald Poirier , René Maltais , Jean-Yves Sancéau , Hassan Fahmi , Mohamed Benderdour *

Posted Date: 22 February 2024

doi: 10.20944/preprints202402.1255.v1

Keywords: Resolvin D1; Analogues, Osteoarthritis; Antioxidant; Reactive Oxygen Species; Hyaluronic Acid

Article

Development of New Resolvin D1 Analogues for Osteoarthritis Therapy: Acellular and Computational Approaches to Study Their Antioxidant Activities.

Zahra Kariminezhad [1], Mahdi Rahimi [1], Julio Fernandes [1], René Maltais [2], Jean-Yves Sancéau [2], Donald Poirier [2,3], Hassan Fahmi [4] and Mohamed Benderdour [1,*]

[1] Orthopedic Research Laboratory, Hôpital du Sacré-Cœur de Montréal, Université de Montréal, Montréal, Qc, Canada.
[2] Department of Molecular Medicine, Faculty of Medicine, Université Laval, Québec, QC, Canada.
[3] Organic Synthesis Service, Medicinal Chemistry Platform, CHU de Québec Research Center-Université Laval, Québec, QC, Canada.
[4] Osteoarthritis Research Unit, University of Montreal Hospital Research Center (CRCHUM), Montreal, QC, Canada
* Correspondence: email: mohamed.benderdour@umontreal.ca; Tel.: (514 338- 2222 #3279)

Abstract: In osteoarthritis (OA), oxidative stress plays a crucial role in maintaining and sustaining cartilage degradation. Current OA management requires a combination of pharmaceutical and non-pharmacological strategies, including intraarticular injections of hyaluronic acid (HA). However, several lines of evidence reported that HA oxidation by reactive oxygen species (ROS) is linked with HA cleavage and fragmentation, resulting in reduced HA viscosity. Resolvin D1 (RvD1) is a lipid mediator that is biosynthesized from omega-3 polyunsaturated fatty acids and is a good candidate with the potential to regulate of panoply of biological processes, including tissue repair, inflammation, oxidative stress, and cell death in OA. Herein, newly designed, and synthesized imidazolium RvD1 analogues were introduced to compare their potential antioxidant properties with commercially available RvD1. Their antioxidant capacities were investigated by several *in vitro* chemical assays including Oxygen Radical Absorbance Capacity, 2,2-Diphenyl-1-picrylhydrazyl Radical Scavenging, Ferric Ion Reducing Antioxidant Power, Hydroxyl Radical Scavenging, and HA Fragmentation Assay. All results proved that imidazolium RvD1 analogues showed excellent antioxidant performance compared to RvD1 due to their structural modifications. Interestingly, they scavenged the formed reactive oxygen species (ROS) and protected HA from degradation, as verified by agarose gel electrophoresis and gel permission chromatography. A computational study using Gaussian 09 with DFT calculations and B3LYP/6-31 G (d, p) basis set was also employed to study the relationship between the antioxidant properties and chemical structures as well as calculation of the molecular structures, frontier orbital energy, molecular electrostatic potential, and bond length. The results showed that the antioxidant activity of our analogues was higher than that of RvD1. In conclusion, the findings suggest that imidazolium RvD1 analogues can be good candidates as antioxidant molecules for the treatment of oxidative stress-related diseases like OA. Therefore, they can prolong the longevity of HA in the knee and thus may improve the mobility of the articulation.

Keywords: Resolvin D1; analogues; osteoarthritis; antioxidant; reactive Oxygen species; hyaluronic acid

1. Introduction

Osteoarthritis (OA) is known as a chronic degenerative and musculoskeletal disorder that causes pain and physical disability in patients' quality of life [1,2]. Although OA is considered a global disease affecting all joint tissues (subchondral bone, ligaments, capsule, synovial membrane, and menisci), cartilage degradation is the end point of this disease [3]. The degradation of cartilage can be started by the combination of mechanical stress and biochemical factors. One of the most important biochemical alterations in OA is oxidative stress, characterized by the increased formation of reactive oxygen species (ROS), reactive nitrogen species (RNS), lipid peroxidation (LPO) products,

 doi:10.20944/preprints202402.1255.v1

and the insufficiency of biological molecules to scavenge these hazardous species [4–7]. ROS/RNS can be classified as either free radicals containing one unpaired electron or nonradicals including superoxide radical ($O2^{\bullet-}$), hydroxyl radical (•OH), NO radical (•NO), peroxyl (ROO•), and alkoxyl radicals (RO•) [8]. At controlled levels, ROS act as signaling molecules in cells. However, an imbalance between ROS and antioxidants, known as redox state dysregulation, disrupts cell function and can contribute to disease. In OA, ROS and LPO accumulation cause cartilage damage by increasing the degradation of the extracellular matrix (ECM) and decreasing the synthesis of proteoglycan and type II collagen [7,9–11]. Hyaluronic acid (HA), a naturally occurring non-sulfated glycosaminoglycanes (GAG), is found in synovial fluid, cell surface, and ECM tissue. It is composed of disaccharides containing glucuronic acid and N-acetylglucosamine which is synthesized by the HA synthase (HAS) [12]. HA is initially present as a polymer with high molecular weight (HMW), but it undergoes degradation by hyaluronidase (HYAL) or ROS/RNS actions leading to broken down into smaller fragments and oligosaccharides with low molecular weight (LMW) [13]. HMW HA has anti-inflammatory, immunosuppressive, and antiangiogenic effects, whereas LMW HA has pro-inflammatory, pro-angiogenetic, and oncogenic effects [14]. ROS/RNS naturally degrades HMW HA, albeit at enhanced levels during tissue injury and inflammatory processes [15,16]. Several HA formulations were developed to protect its oxidation and degradation. These formulations include the combination of HA with sorbitol and mannitol. These compounds can prolong the longevity of injected HA in the knee and thus may improve the mobility and flexibility of the articulation [17–20]. At the cellular level, these formulations restore redox status and reduce markers of apoptosis, inflammation and catabolism involved in cartilage damage [21,22]. Thus, the degradation of HA by increased ROS challenges vascular integrity and can initiate OA disease progressions (Figure 1).

Growing evidence implicates ROS pathways in the development of osteoarthritis. Leveraging this knowledge, researchers are exploring innovative antioxidant-based interventions. These interventions aim to reduce harmful oxidative stress and bolster cellular defenses, potentially paving the way for innovative OA management strategies [23]. Enzymatic and non-enzymatic antioxidants are responsible for controlling and inhibiting oxidative enzymes, scavenging free radicals, or chelating ion metals [24]. There are two complementary antioxidant defense systems against oxidative stress: the enzymatic system (SOD, GPX, CAT) catalyzes ROS conversion, while the non-enzymatic system (GSH, vitamin C, vitamin E, carotenoids) directly quenches ROS or participates in redox cycles [25]. Antioxidants, derived from both endogenous and exogenous sources, exert crucial functions in free radical scavenging, prevention, and neutralization of pre-radical molecules. The development of antioxidant-based supplements and drugs offers a potential avenue for reinforcing cellular antioxidant status and mitigating the detrimental effects of oxidative stress. Resolvins are a class of compounds derived from omega-3 fatty acids and subclassed in three categories including Resolvin Ds, Resolvin Es, Resolvin Ts, Resolvin-3DPA, and Resolvin-6DPA [26,27]. Among these, Resolvin D1 (RvD1) has been suggested as a novel treatment option for several inflammatory diseases due to its remarkable properties in resolving inflammation, promoting tissue repair, preserving tissue integrity, treatment of bone and cartilage disorders [28–33]. However, RvD1 is a chemically unstable molecule that undergoes a very fast transformation to inactive products through the enzymatic action of eicosanoid oxidoreductase [34,35]. To improve this instability, research has been studied to develop and synthesize metabolically stable analogues with improved pharmacokinetic and pharmacodynamic properties.

Very recently, our research team designed and synthesized a series of RvD1 analogues and conducted several biological studies to present their abilities to inhibit inflammatory processes and antioxidant properties [36]. Herein, we performed *in vitro* assays to measure the antioxidant capacity of newly designed imidazolium RvD1 analogues and simulated their activity by computational study. In this regard, oxygen radical absorbance capacity (ORAC) and hydroxyl radical scavenging with copper II (HRS), 2,2-diphenyl-1-picrylhydrazyl (DPPH), and ferric reducing antioxidant power (FRAP) assays were performed to measure the total antioxidant status and determine the antioxidant activity of analogous. The effectiveness of imidazolium RvD1 analogues in scavenging radicals was evaluated by incubating HMW HA, an important component of cartilage and synovial fluid, with

 doi:10.20944/preprints202402.1255.v1

ROS. The protection of HMW HA from degradation was checked by agarose gel electrophoresis and gel permeation chromatography. Moreover, the quantum chemical simulation was used to characterize the molecular structure, and the density functional theory (DFT) study provided useful data related to antioxidant capacity such as O-H bond length, chemical reactivity, and energy of frontier orbitals. DFT study was also performed to analyze the antioxidant activity and the active sites of RvD1 and its analogues.

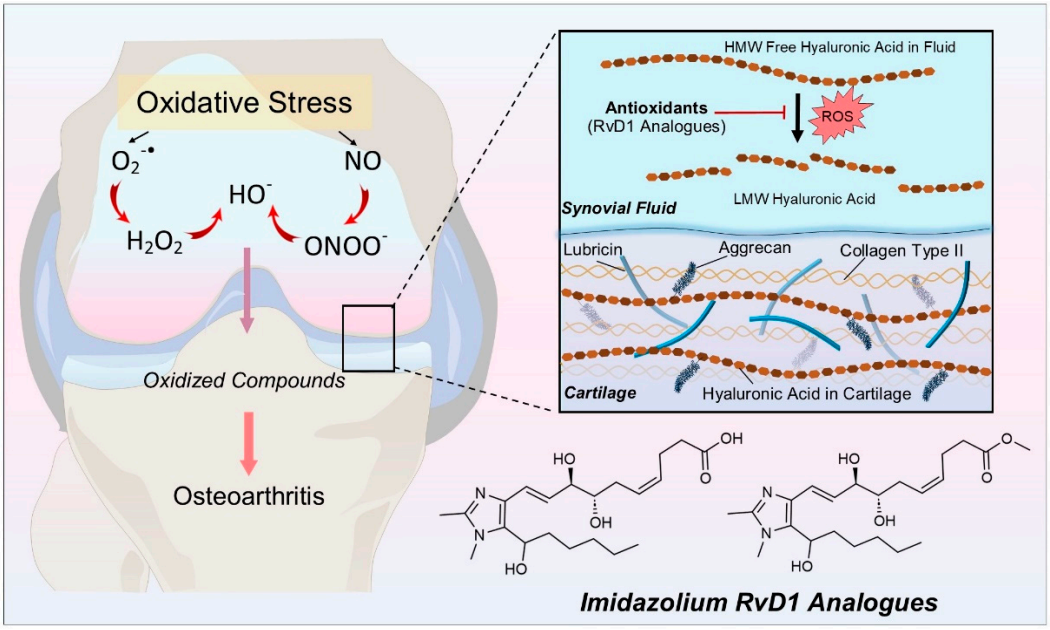

Figure 1. Oxidative stress and its mechanism in osteoarthritis; The primarily formed radicals, superoxide radical ($O^{2-\bullet}$), can be converted to more harmful species such as hydroxyl radicals ($OH^{\bullet}$) and hydrogen peroxide (H_2O_2). Imidazolium RvD1 analogues as antioxidant molecules scavenge ROS via their active sites to protect against the degradation of high molecular weight hyaluronic acid (HMW HA) to low molecular weight hyaluronic acid (LMW HA).

2. Materials and Methods

2.1. Materials

Chemical reagents including fluorescein sodium salt (NaFluo, BioReagent), 2,2′-azobis(2-methylpropionamidine) dihydrochloride (AAPH, granules, 97%), and 2,2-diphenyl-1-picrylhydrazyl (DPPH, powder) were purchased from MilliporeSigma Co. The antioxidants as controls including ascorbic acid (AA, 99%) and (±)-6-hydroxy-2,5,7,8-tetramethylchromane-2-carboxylic acid (Trolox, 97%) were also obtained from MilliporeSigma Co. Ferric Reducing Antioxidant Power (FRAP) Assay Kit (Colorimetric) was purchased from Invitrogen by Thermo Fisher Scientific (REF. EIAFECL2). Resolvin D1 was purchased from Cayman Chemical Co. and stored at -80°C. Two Imidazolium Resolvin D1 analogues including (4Z,7R,8R,9E)-7,8-dihydroxy-10-(5-(1-hydroxyhexyl)-1,2-dimethyl-1H-imidazol-4-yl)deca-4,9-dienoic acid (Analogue 1) and methyl (4Z,7S,8R,9E)-7,8-dihydroxy-10-(5-(1-hydroxyhexyl)-1,2-dimethyl-1H-imidazol-4-yl)deca-4,9-dienoate (Analogue 2) were synthetized by Poirier' research group. The purity of the final compounds RvD1 analogues 1 and 2 to be tested was determined with a Shimadzu HPLC apparatus equipped with an SPD-M20A photodiode array detector, a Setima HPLC18 reversed-phase column (250 mm × 4.6 mm) and using a solvent gradient of MeOH:water from 70:30 to 100:0 on 30 min run. The wavelength of the UV detector was 245 nm.

2.2. Analogues synthesis

2.2.1. Block A synthesis

 doi:10.20944/preprints202402.1255.v1

The **block A** synthesis sequence was adapted from Gaetano et al. [37].

(i) 2-deoxy-3,4-*O*-(1-methylethylidene)-D-*erythro*-pentopyranose (**1**)

To a solution of 2-desoxy-D-ribose (18.7 mmol, 2.5 g) in anhydrous DMF (25 mL) under an argon atmosphere was added dierite dessicant (1.0 g), dimethoxy-propane (37 mmol, 3.8 g, 4.5 mL) and p-TSA (0.55 mmol, 0.1 g). The solution was stirred 3 h at room temperature. Triethylamine (TEA) (0.1 mL) was then added before to be filtered over celite pad. The filtrate was evaporated under pressure. The crude compound was purified by flash chromatography with EtOAc/Hexanes (7:3 + 1% TEA) to give 1.7 g (53 %) of compound **1**. ^{1}H NMR spectra was in full agreement with literature data.

(ii) (Methoxycarbonyl propyl)triphenylphosphonium bromide (**2**)

To a solution of methyl-4-bromo-butanoate (25.0 g, 140 mmol) in toluene (250 mL) was added triphenylphosphine (33.5 g, 170 mmol) and stirred at 100°C for 24 h. The resulting solid was then filtered and washed with cold toluene to give compound **2** as a white solid (12.0 g, 20%).

(iii) Methyl (4*Z*)-6-[(4*S*,5*R*)-5-(hydroxymethyl)-2,2-dimethyl-1,3-dioxolan-4-yl]hex-4-enoate (**3**)

To a solution of phosphonium salt **2** (9.6 g, 21 mmol) in anhydrous THF (60 mL) at -78 °C under an argon atmosphere was dropwise added KHMDS (1.0 M in THF, 20 mmol, 20.0 mL) over 10 min. The solution was then allowed to return at 0°C and was stirred for 1 h. To the later solution cooled down at -78°C was added compound **1** (1.5 g, 8.7 mmol) and stirred 20 min at this temperature before to be warmed at room temperature and stirred for an additional 30 min. The resulting solution was poured into a saturated ammonium chloride solution and extracted with EtOAc. The organic layer was washed with brine, dried over sodium sulfate, filtered, and evaporated under reduced pressure. The resulting crude compound was purified by flash chromatography with EtOAc/Hexanes (1:1 + 1% TEA) to give 0.67 g (32%) of compound **3**. ^{1}H NMR spectra was in full agreement with literature data.

(iv) Methyl (4*Z*)-6-[(4*S*,5*S*)-5-formyl-2,2-dimethyl-1,3-dioxolan-4-yl]hex-4-enoate (**4**)

To a solution of compound **3** (2.8 mmol, 0.67 g) in dichloromethane (DCM) (10 mL) was dropwise added a solution of Dess-Martin periodinane (5.6 mol, 2.4 g) in 10 mL of DCM. The solution was stirred for 2 h and then poured into a saturated solution of sodium bisulfite. The solution was then extracted with EtOAc. The organic layer was washed with a saturated solution of sodium bicarbonate, and then with brine, dried with sodium sulfate, filtered and evaporated under reduce pressure. The resulting crude product **4** was used as such toward next step. ^{1}H NMR spectra was in full agreement with literature data.

(v) methyl (4*Z*)-6-[(4*S*,5*R*)-5-ethynyl-2,2-dimethyl-1,3-dioxolan-4-yl]hex-4-enoate (**5**)

To K_2CO_3 (7.9 mmol, 1.1 g) under an argon atmosphere was dropwise added a solution of phosphonate (3.9 mmol, 0.67 g) in MeOH (10 mL). To the later solution was dropwise added a solution of aldehyde **4** (2.8 mmol, 0.67 g) in MeOH (45 mL) at room temperature and the solution was stirred for 3 h at room temperature. The resulting solution was poured into water, extracted with EtOAc, washed with brine, dried over sodium sulfate, filtered and evaporated under reduce pressure. The crude compound was purified by flash chromatography with EtOAc/hexanes (3:7 + 1% TEA) to give 330 mg (50%) of compound **5**. ^{1}H NMR (400 MHz, Acetone- d_6) 5.57 – 5.36 (m, 2H), 4.77 (dd, *J* = 5.5, 2.2 Hz, 1H), 4.10 (ddd, *J* = 7.2, 6.5, 5.5 Hz, 1H), 3.59 (s, 3H), 3.05 (d, *J* = 2.2 Hz, 1H), 2.56 – 2.42 (m, 2H), 2.42 – 2.26 (m, 2H), 1.43 (s, 3H), 1.26 (s, 3H).^{13}C NMR (100.6 MHz, Acetone-d_6) 172.7, 130.1, 125.8, 110.0, 109.3, 77.4, 76.3, 68.8, 50.7, 33.3, 29.4, 27.2, 25.6, 22.8 ppm. LRMS (APCI pos) *m*/*z* 253.1 [M + H].

(vi) Methyl (4*Z*)-6-{(4*S*,5*R*)-2,2-dimethyl-5-[(*E*)-2-(4,4,5,5-tetramethyl-1,3,2-dioxaborolan-2-yl)ethenyl]-1,3-dioxolan-4-yl}hex-4-enoate (**Block-A**)

In a microwave vial under an argon atmosphere was added compound **5** (1.3 mmol, 330 mg), TEA (0.4 mmol, 0.04 mL) and pinacolborane (2.5 mmol, 0.38 mL). At this mixture was added the Schwartz reagent (0.13 mmol, 34 mg) and the solution was heated at 60°C for 36 h. The resulting solution was poured into water, extracted with EtOAc, washed with brine, dried over sodium sulfate, filtered and evaporated under reduce pressure. The crude compound was purified by flash chromatography with EtOAc/hexanes (2:8 + 1% TEA) to give 105 mg (21%) of compound **Block-A**. ^{1}H NMR (400 MHz, Acetone- d_6)) δ 6.60 – 6.39 (m, 1H), 5.64 (dd, *J* = 18.0, 1.4 Hz, 1H), 5.44 – 5.33 (m, 2H), 4.58 (td, *J* = 6.4, 1.4 Hz, 1H), 4.23 (dt, *J* = 7.7, 6.3 Hz, 1H), 3.58 (s, 3H), 2.41 – 2.24 (m, 4H), 2.18 (td, *J* = 7.4, 6.7, 4.5 Hz, 2H), 1.41 (d, *J* = 0.7 Hz, 3H), 1.28 (d, *J* = 0.7 Hz, 3H), 1.22 (s, 12H).^{13}C NMR (100.6

 doi:10.20944/preprints202402.1255.v1

MHz, Acetone-d_6) 172.6, 148.8, 129.6, 126.5, 108.0, 83.0, 79.8, 77.9, 50.7, 33.3, 27.5, 24.8, 24.2, 22.9 ppm. LRMS (APCI pos) *m/z* 381.2 [M + H].

2.2.2. Block B synthesis

The **block B** was prepared following a literature procedure [37], as shown in Figure 2. Briefly, 1,2-dimethylimidazole was treated with N-bromosuccinimide (2.2 eq) in chloroform and reacted for 14 h at room temperature to give the dibromo-imidazole compound – **Block B.** Reaction was quenched and compound isolated and/or purified. ^{1}H NMR data were in full agreement with that reported in the literature.

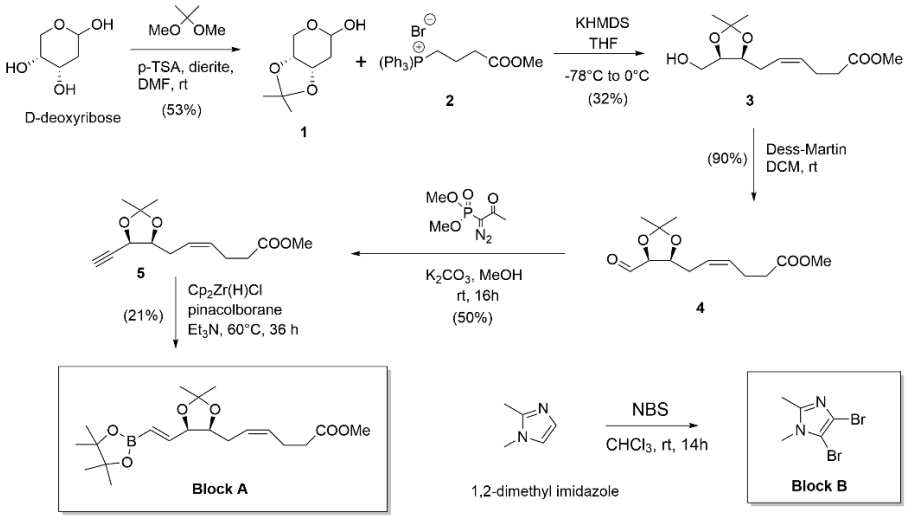

Figure 2. Chemical synthesis of **Block A** and **Block B**. Reagents, conditions and reaction yields.

2.2.3. RvD1 analogues 1 and 2 syntheses

*(i) 1-(4-bromo-1,2-dimethyl-1H-imidazol-5-yl)hexan-1-one (**6**)*

This compound was prepared following a literature procedure [37] (Figure 3). ^{1}H NMR data were in full agreement with that reported in the literature.

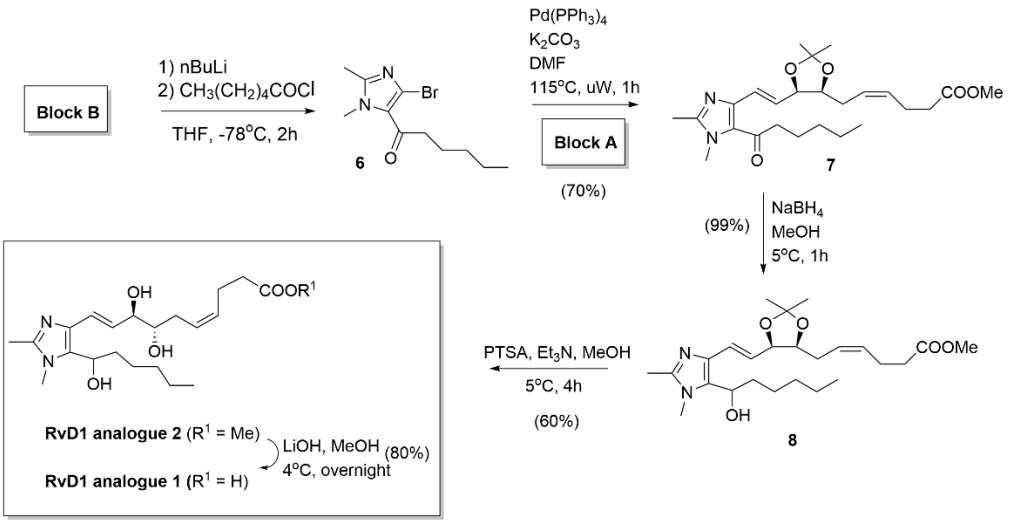

Figure 3. Chemical synthesis of **RvD1 analogues 1** and **2**. Reagents, conditions and reaction yields.

*(ii) Methyl (4Z)-6-{(4S,5R)-5-[(E)-2-(5-hexanoyl-1,2-dimethyl-1H-imidazol-4-yl)ethenyl]-2,2-dimethyl-1,3-dioxolan-4-yl}hex-4-enoate (**7**)*

 doi:10.20944/preprints202402.1255.v1

In a 20 mL microwave vial, compound **6** (54 mg, 0.20 mmol) and Block **A** (100 mg, 0.26 mmol) were solubilised in DMF (1.2 mL) and 2M K_2CO_3 (0.2 mL). Argon was bubbled through the mixture for 15 min before addition of $Pd(PPh_3)_4$ (20 mg. 0.016 mmol). After sealing, the tube was heated in a microwave apparatus at 115°C for 1 h. After cooling at room temperature, water was added and the aqueous phase extracted with EtOAc. The combined extracts were washed with water, brine and dried over Na_2SO_4. The residue was purified on silica gel eluting with toluene-EtOAc-ether (90:10:10 to 70:30:10) affording compound **7** (61 mg, 70%). ^{1}H NMR shows contamination with triphenylphosphine oxide and (1,2-dimethyl-1H-imidazol-5-yl)hexan-1-one. ^{1}H NMR (400 MHz, Methanol-d_4) δ 6.86 (d, J = 15.3 Hz, 1H), 6.43 (dd, J = 15.3, 6.8 Hz, 1H), 5.33 (m, 2H), 4.68 (m, 1H), 4.21 (q, J = 6.6 Hz, 1H), 3.65 (s, 3H), 3.49 (s, 3H), 2.29 (s, 3H), 2.18 (s, 6H), 1.58 (m, 2H), 1.41 (s, 3H), 1.26 (m, 7H), 0.81 (bs, 3H).

*(iii) Methyl (4Z)-6-[(4S,5R)-5-{(E)-2-[5-(1-hydroxyhexyl)-1,2-dimethyl-1H-imidazol-4-yl]ethenyl}-2,2-dimethyl-1,3-dioxolan-4-yl]hex-4-enoate (**8**)*

To an ice-cooled solution of compound **7** (60 mg, 0.13 mmol) in MeOH (1 mL) was added $NaBH_4$ (10 mg, 0.26 mmol). The mixture was stirred at 5°C for 1 h then quenched with a 10% aqueous solution of NaH_2PO_4. The aqueous phase was extracted twice with EtOAc. The combined extracts were washed with water, brine and dried over Na_2SO_4. Evaporation gave quantitatively compound **8** (60 mg). ^{1}H NMR (400 MHz, Methanol-d_4) δ 6.59 (d, J = 15.6 Hz, 1H), 6.21 (dd, J = 15.6, 8.1 Hz, 1H), 5.43 (m, 2H), 4.68 (m, 1H), 4.21 (m, 1H), 3.65 (s, 3H), 3.62 (s, 3H), 2.30 (s, 3H), 2.18 (s, 3H), 1.92 (m, 1H), 1.76 (m, 1H), 1.49-1.19 (m, 6H), 0.88 (bs, 3H).

*(iv) Methyl (4Z,7S,8R,9E)-7,8-dihydroxy-10-[5-(1-hydroxyhexyl)-1,2-dimethyl-1H-imidazol-4-yl]deca-4,9-dienoate (**RvD1 analogue 2**)*

To a solution of crude compound **8** (60 mg, 0.13 mmol) in MeOH (1 mL) was added p-TSA (39 mg, 0.21 mmol) at 5°C and stirred for 4 h. Triethylamine was added and MeOH was evaporated under reduce pressure. The residue was poured into water and extracted with EtOAc. The combined extracts were washed with water, brine, dried over Na_2SO_4, filtered and evaporated under reduced pressure to give crude material. This later compound was purified by flash chromatography using DCM/MeOH (9:1) as eluent to give compound **RvD1 analogue 2** (33 mg, 60%). ^{1}H NMR (400 MHz, Methanol- d_4) δ 6.58 (d, J = 15.7 Hz, 1H), 6.27 (dd, J = 15.1, 7.3 Hz, 1H), 5.55 (m, 2H), 5.45 (m, 1H), 4.58 (m, 1H), 4.08 (m, 1H), 3.64 (s, 3H), 3.59 (s, 3H), 2.37 (m, 3H), 1.93-1.71 (m, 2H), 1.49-1.17 (m, 6H), 0.88 (bs, 3H). ^{13}C NMR (100.6 MHz, Methanol- d_4) 174.0, 146.0, 149.9, 133.5, 130.1, 128.9, 127.4, 127.2, 126.6, 126.5, 121.6, 75.5, 75.4, 74.6, 74.5, 64.9, 50.6, 36.1, 36.0, 33.4, 33.3, 31.4, 31.3, 30.7, 30.2, 25.5, 25.4, 22.6, 22.3, 12.9, 11.2. LRMS (APCI pos) *m/z* 409.3 [M + H]. HPLC purity = 99.6%.

*(v) (4Z,7S,8R,9E)-7,8-dihydroxy-10-[5-(1-hydroxyhexyl)-1,2-dimethyl-1H-imidazol-4-yl]deca-4,9-dienoic acid (**RvD1 analogue 1**)*

To a solution of compound **RvD1 analogue 2** (22 mg, 0.06 mmol) in MeOH (0.5 mL) was added LiOH (16 mg, 0.38 mmol). The mixture was stirred at 4°C overnight and then poured into aqueous solution (10%) of NaH_2PO_4. The aqueous solution was extracted with EtOAc, washed with brine, dried over sodium sulfate, filtered and evaporated under reduce pressure to give 17 mg (80%) of compound **RvD1 analogue 1** as a yellow solid. ^{1}H NMR (400 MHz, Methanol- d_4) δ 6.65 (d, J = 15.7 Hz, 1H), 6.42 (dd, J = 15.1, 7.3 Hz, 1H), 5.51 (m, 2H), 4.94 (m, 1H), 4.18 (m, 1H), 3.75 (s, 3H), 3.65 (m, 1H), 2.51 (s, 3H), 2.47-2.38 (m, 2H), 2.38-2.23 (m, 4H), 1.93-1.77 (m, 2H), 1.49-1.19 (m, 6H), 0.90 (bs, 3H). ^{13}C NMR (100.6 MHz, Methanol- d_4) 177.2, 145.6, 145.5, 130.9, 130.8, 130.2, 130.1, 129.9, 129.3, 126.4, 126.1, 117.5, 117.4, 74.43, 74.41, 74.4, 74.3, 64.7, 64.6, 35.96, 35.9, 34.8, 31.33, 31.32, 31.3, 30.4, 30.3, 29.3, 25.34, 25.33, 23.3, 22.2, 12.9, 10.1, 10.0. LRMS (APCI pos) *m/z* 395.3 [M + H]. HPLC purity = 100.0%.

All results of analogues synthesis, including ^{1}H NMR spectrum, ^{13}C NMR spectrum, LCMS chromatogram, and mass spectrum, were described in Figures S1-9.

2.3. Antioxidant Activity Assays

2.3.1. Oxygen Radical Absorbance Capacity (ORAC) Assay

 doi:10.20944/preprints202402.1255.v1

The ORAC assay was performed as described by Huang et al. with the following modifications [38]. Briefly, different concentrations of antioxidant samples were prepared in phosphate buffer solution (PBS 75 mM, pH 7.4). Then, a fresh stock solution of fluorescein (58 nM) in PBS was prepared in a separate conical tube and stored at 4 °C. Afterward, 20 µL of different concentrations of antioxidants were mixed with 120 µL of fluorescein probe in a 96-well plate and incubated at 37 °C for 30 min. The fluorescence intensity (excitation. 485 nm, emission. 520 nm) was measured to determine the background signal by fluorometer. Subsequently, 60 µL of 2,2'-azobis(2-methylpropionamidine) dihydrochloride (AAPH) (40 mM) was added manually with a multichannel pipette for all wells except for the negative control (fluorescein probe without AAPH). The plate was scanned for 250 cycles every 60 seconds. The final concentrations of the antioxidants in the wells are as follows; 20, 10, 5, 2.5, 1.25, and 0.625 µM. The area under the curve (AUC), and the Net AUC for all samples and standards were measured using Equations 1 and 2, respectively.

$$AUC = (R_1/R_1) + (R_2/R_1) + (R_3/R_1) + \cdots + (R_n/R_1) \quad (1)$$

R_1= relative fluorescence value of time points zero.

R_n= relative fluorescence value of time points (e.g., R_3 is relative fluorescence value at minute=3).

$$NET\ AUC = AUC_{Antioxidant} - AUC_{Blank} \quad (2)$$

The standard curve was obtained by plotting the Net AUC against the concentrations of different antioxidant samples. For comparison of the data, the antioxidant activity of all samples was converted into Trolox Equivalent (TE) according to Equation 3.

$$TE = Slope_{Sample}/Slope_{Trolox} \quad (3)$$

2.3.2. DPPH Assay

2,2-Diphenyl-1-picrylhydrazyl (DPPH) method was performed according to the discovered method by Goldschmidt and Renn in the 1920s and then developed by Blois in 1958 [39,40]. Firstly, different concentrations of antioxidants were prepared in deionized water. Then, in a separate conical tube, a fresh stock solution of DPPH reagent (600 µM) was prepared in methanol and stored at 4 °C. In a 96-well plate, 50 µL of different concentrations of antioxidants were mixed gently with 50 µL of DPPH solution and incubated in a dark condition at room temperature for 30 min. The well containing DPPH without antioxidants is considered as a negative control and the final concentrations of the antioxidants in the wells are as follows; 20, 10, 5, 2.5, 1.25, and 0.625 µM. The absorbance was measured by an ELISA microplate reader at 517 nm. The scavenging percentage of all samples was measured using Equation 4.

$$DPPH\ Scavenging\% = [(Abs_{control} - Abs_{sample}) / (Abs_{control})] \times 100 \quad (4)$$

2.3.3. FRAP Assay

The Ferric Reducing Antioxidant Power (FRAP) assay was developed by Iris Benzie and J.J. Strain [41]. To determine the antioxidant activity of the samples, the experiment procedure was done according to the protocol provided by the manufacturer. In a 96-well plate, 25 µL of standards or different concentrations of samples were mixed with 75 µL FRAP color solution and incubated at room temperature for 30 minutes. The final concentrations of the antioxidants in the wells were as follows; 20, 10, 5, 2.5, 1.25, 0.625, and 0.3125 µM. Subsequently, the absorbance was read at 593 nm by UV spectrophotometer. According to the FRAP kit protocol, a serial dilution of ferrous chloride ($FeCl_2$) standard was prepared in assay buffer 1X (provided by FRAP kit) to plot the calibration curve.The relative percentage of reducing power in compared Trolox for all antixodants samples were calculated according to the following formula [42].

$$Relative\ \%\ of\ Reducing\ Power = (Abs_{samaple} - Abs_{min}) / Abs_{max} - Abs_{min}) \times 100 \quad (5)$$

Where, Abs - absorbance of sample, Abs_{min} – Absorbance of control, and Abs_{max} - Highest Abs of control (Trolox).

 doi:10.20944/preprints202402.1255.v1

2.3.4. Hydroxyl Radical Scavenging (HRS)

The Hydroxyl Radical Scavenging activity of RvD1 and analogues was performed in 96-well black plate in the presence of $CuCl_2$ and H_2O_2 in acellular conditions [43]. Briefly, 10 µM $CuCl_2$ and 100 µM H_2O_2 were mixed in 100 µL/well of PBS (75 mM, pH 7.4) in the presence or absence of RvD1, Analogue 1, Analogue 2, Trolox at a concentration of 10 µM. Then after, 100 µL of DCFH-DA probe solution were added to each well in a final concentration of 20 µM. The fluorescence was measured at 0, 0.5, 1, 2, 4, and 8 h after exposure time, using a microplate reader with fluorescence polarization (Polar Star Optima, BMG Labtech) set up at excitation wavelengths of 485 nm and emission wavelength of 530 nm. The results were expressed as relative fluorescence units (RFU).

2.4. Hyaluronic Acid Degradation Study

The hyaluronic acid degradation assay was peroformed as described by Chen et al [43] with minor modifications. Briefly, a solution of HA at 1 mg/mL was treated with 10 µM $CuCl_2$, 100 µM H_2O_2 in the presence or absence of Trolox, RvD1, or analogues at a final concentration of 10 µM. The reaction was conducted in 37°C during 16 h. 20 µg of HA were loadded into an agarose gel (2% prepared in TBE buffer) using a loading buffer containing 0.25% of bromophenol blue solubilized in formamide. After 4 h of migration at 40 volts, the HA was visualized after staining with Stain-All dissolved in 30% ethanol.

2.5. Hyaluronic Acid Analysis by Gel Permeation Chromatography

Gel permeation chromatography/size exclusion chromatography) (GPC/SEC) measurements were performed by Two AquaGel columns (PAA-202 + PAA-206M) connected in series (PolyAnalytik, London, Canada) using a Viscotek TDA305 and GPCmax. It is equipped with an oven that houses three detectors: Refractive Index (RI), Right Angle and Low Angle Light Scattering (RALS/LALS), and Four-Capillary Differential Viscometer. The measurements were carried out in 8.5g/L NaCl in MiliQ as mobile phase, at a flow rate of 0.7 mL/min at 30 °C. PEG 20 kDa (dn/dc = 0.132 mL/g) and dextran 72 kDa (dn/dc = 0.147 mL/g) with a concentration of 3 mg/mL were used as standards for the determination of the calibration curve. The samples were diluted using mobile phase to a concentration of approximately 0.25 mg/mL and filtered with 0.22 µm Nylon syringe filters prior to injection. The sample concentration was approximately 2 mg/mL and the injection load was 100 µL.

2.6. Computational Studies

This study was carried out using the Gaussian 09 software package. The ground-state geometry optimization of antioxidants was done with DFT using the B3LYP/6-31 + G (d, p) to obtain the minimum on the potential energy surface. The plotting of the three-dimensional mapping of the molecular orbitals and the highest occupied molecular orbital (HOMO) and lowest unoccupied molecular orbital (LUMO) energies were calculated using the B3LYP/6-31 + G (d, p) basis set.

3. Results and Discussion

3.1. Antioxidants and Radical Scavenging Activities of Resolvin Analogues

3.1.1. ORAC Assay

Several *in vitro* chemical assays have been developed and reviewed for measuring antioxidant capacity. The complicated mechanism among free radicals, substrates, and antioxidants makes it impossible to present an equation to express the kinetic order. Accurate quantification of antioxidant potential mandates the consideration of both inhibition degree, denoting the extent of free radical scavenging, and inhibition time, reflecting the persistence of the antioxidant effect. In this regard, the oxygen radical absorbance capacity (ORAC) assay stands out as the sole technique currently available that effectively integrates these complementary parameters into a single, informative value. Thus,

 doi:10.20944/preprints202402.1255.v1

this method is widely used in the nutraceutical, pharmaceutical, food industries, and biomedical studies [38]. In this assay, a radical-generating compound, 2,2′-azobis(2-amidinopropan) dihydrochloride (AAPH), produces biologically relevant oxygen radical species (ROS) via thermal decomposition in the presence of oxygen. As the ROS oxidizes the fluorescein, the fluorescence of the solution decreases over time. In the presence of an antioxidant, ROS can be scavenged, and the oxidation of fluorescein can be delayed until the antioxidant is depleted. Indeed, antioxidants protect fluorescein from ROS attacking by the way of hydrogen atom transfer (HAT) process (Figure 4).

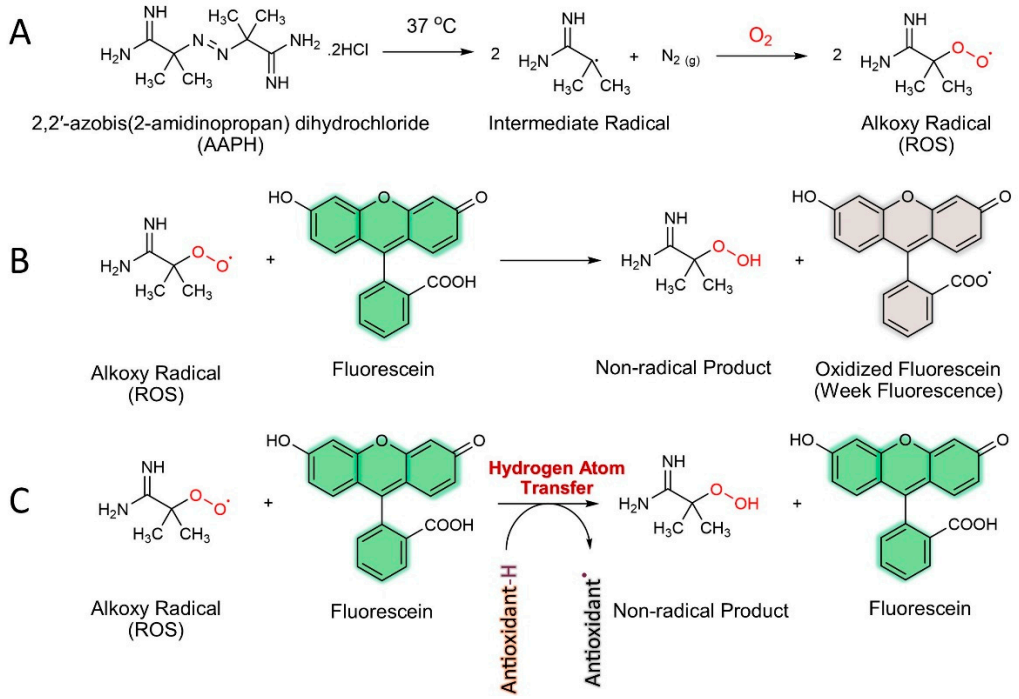

Figure 4. ORAC assay mechanism; (A) Generating ROS (alkoxy radical) by thermal decomposition of 2,2′-azobis(2-amidinopropan) dihydrochloride (AAPH) in the presence of oxygen. (B) Reacting ROS with fluorescein (fluorescent probe) without antioxidant compounds and production of non-fluorescent molecule. (C) Inhibition of ROS by antioxidants and protection of fluorescein from radical attack.

In Figure 5, the typical time-dependent decays of fluorescence intensity of fluorescein induced by AAPH alone, or in the presence of antioxidants (final concentration range between 0.625 to 20 μM) were illustrated. After pre-incubation of fluorescein with different concentrations of the antioxidants (including Analogue 1, Analogue 2, RvD1, Ascorbic acid, and Trolox), dose-dependent inhibitions of the fluorescence decay were monitored. As seen in Figure 5A–E, both Analogues 1 and 2 showed the ability of free radical quenching in the radical propagation cascade. According to their shape of fluorescence decay curves, there is no clear distinction between lag time and fluorescein decay periods by increasing the concentrations of the Analogues indicating more complex scavenging kinetics. On the other hand, a very low change was observed for RvD1 by increasing the concentrations which means low scavenging kinetics at the tested condition (Figure 5C). Ascorbic acid and Trolox as controls were also tested to compare the antioxidant capacity of the samples. Although Ascorbic acid is a very strong antioxidant molecule, as seen in Figure 5D, it has a relatively low decay of fluorescence intensity at the tested concentration ranges. Trolox as another control showed a clear lag time proving that it has antioxidant properties to protect fluorescein from ROS (Figure 5E). As a blank control, fluorescein was exposed to excitation light at 485 nm in the absence of AAPH and antioxidants during the assay. The results proved that there is no significant fluorescence intensity change, thus, fluorescein is a stable fluorescent probe according to the analysis.

 doi:10.20944/preprints202402.1255.v1

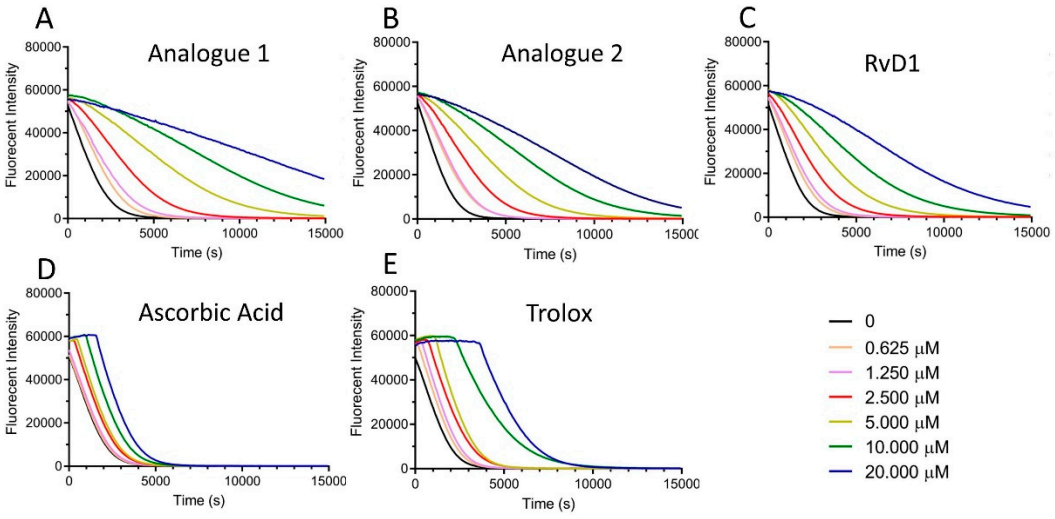

Figure 5. Signal curves for different antioxidant concentrations (0.625 to 20 μM) at 37 °C (Normalized to initial fluorescence signals after AAPH addition).

The antioxidant capacity correlates to the fluorescence decay curve, which is usually represented as the area under the curve (AUC) and calculated according to Equation 1. ORAC calibration curves are depicted in Figure 6 where Net AUC values were plotted against antioxidant concentrations. Trolox equivalent (TE) is a factor that presents the antioxidant capacity compared to Trolox as a standard. Based on this factor, both analogues have better antioxidant capacity compared to other tested antioxidants. Table 1 summarizes the ORAC values of all the samples expressed as μM concentration of Trolox equivalent.

Analogue 1 > Analogue 2 > RvD1 > Trolox > Ascorbic acid

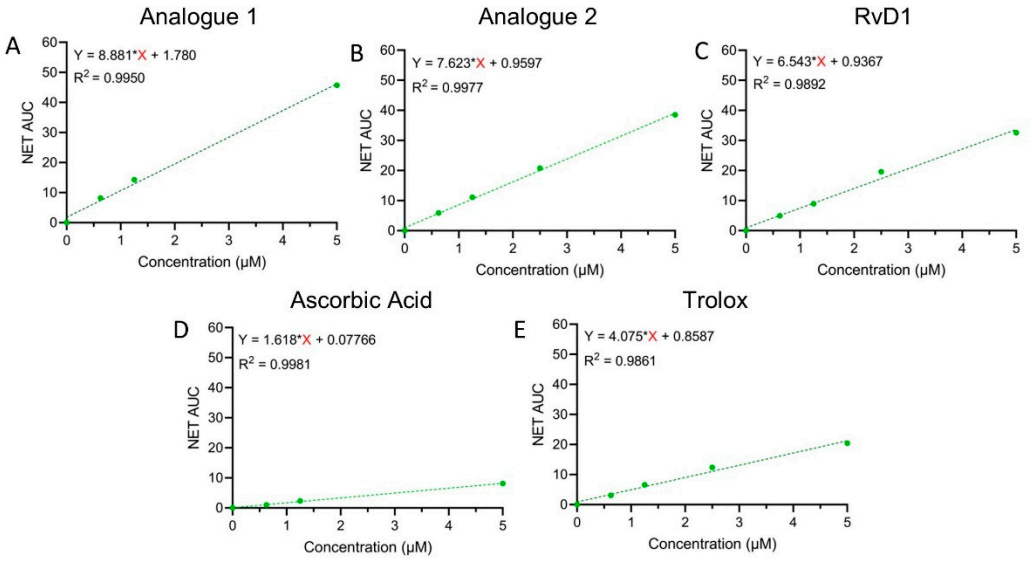

Figure 6. ORAC calibration curves for Analogue 1 (A), Analogue 2 (B), RvD1 (C), Ascorbic acid (D), and Trolox (E).

Table 1. The Trolox Equivalent (TE) values for antioxidant samples.

Antioxidant	Analogue 1	Analogue 2	RvD1	Ascorbic acid	Trolox
TE Value	2.17	1.87	1.60	0.40	1

 doi:10.20944/preprints202402.1255.v1

3.1.2. DPPH Assay

DPPH assay is one of the well-known and routinely practiced assessments of the free radical scavenging potential of antioxidant molecules since it is simple, quick, and relatively inexpensive. It is considered one of the standard and easy colorimetric methods for the evaluation of the antioxidant properties of pure compounds. This assay is based on the reduction of DPPH• free radicals by antioxidant species accepting either a hydrogen atom or an electron (Figure 7). DPPH reagent is considered a stable radical and has limited similarities with peroxyl radicals [44]. Its stability originates from the delocalization of unpaired electrons on a nitrogen atom in the aromatic ring (diphenylamino group as an electron donor, and picryl as an electron acceptor). In this way, the DPPH radical does not dimerize like many other free radicals. The limited space surrounding the nitrogen atom sterically hinders the addition of bulky radicals to this region. Thus, the complex molecules with hydrogen donating sites (like RvD1 and its analogues) cannot approach the nitrogen atom and release the hydrogens there to the formation of hydrazine [45,46]. Since this assay is a colorimetric method, the reduction form of DPPH• free radical (DPPH-H) can be followed by turning purple to a yellow color.

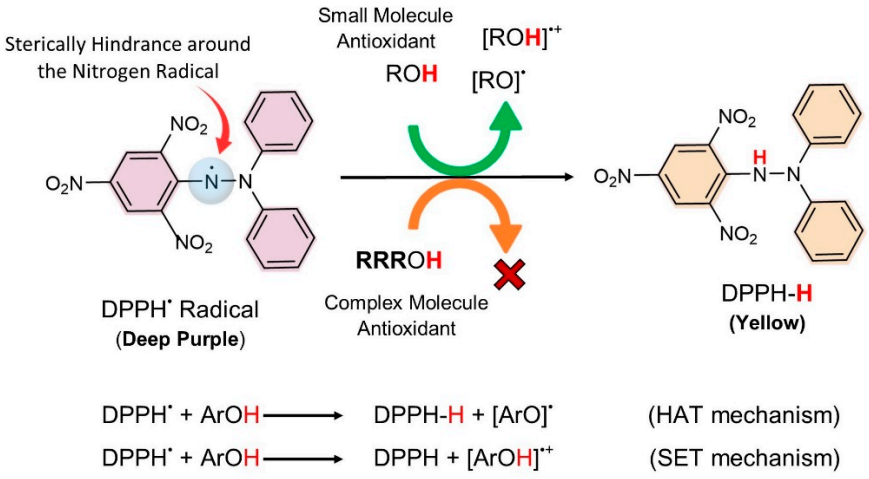

Figure 7. Reaction mechanism of 2,2-diphenyl-1-picrylhydrazyl (DPPH) with two different types of antioxidants (small molecules and complex molecules) via hydrogen atom transfer (HAT) or single electron transfer (SET). Low possibility of interaction between complex molecules and DPPH radical due to the steric hindrance around the radical.

As all samples showed antioxidant activity in the ORAC assay at the range of 0.625-20 μM, the same range concentration was also chosen for the DPPH assay. Both control samples, Ascorbic acid and Trolox showed low scavenging percentages of 4.31±2.74 and 3.53±1.88 μM at 20 μM, respectively, whereas RvD1, Analogue 1, and Analogue 2 did not show any radical scavenging properties under the same conditions. To find the half-maximal inhibitory concentration (IC_{50}) value of the samples, higher concentrations in the range of 20-80 μM were also tested. IC_{50} refers to the antioxidant concentration that scavenges 50% of the initial DPPH radicals in a specific but arbitrary time interval. The color change was monitored spectrophotometrically and utilized for the determination of parameters for antioxidant properties. In the cases of Ascorbic acid and Trolox, the purple color was changed to yellow with a concomitant decrease in absorbance at 515 nm. The IC_{50} value was obtained for Ascorbic acid and Trolox around 66.87 μM and 67.13 μM, respectively. On the other hand, no radical scavenging was observed for RvD1, Analogue 1, and Analogue 2 even at higher concentrations.

It has been proved that some chemicals easily react with DPPH radicals by electron transfer or by donating hydrogen atoms. Especially phenolic compounds are the most reactive and important ones that react easily with DPPH• [47]. For instance, Trolox has a hydroxyl group on the aromatic

 doi:10.20944/preprints202402.1255.v1

ring, which shows good antioxidant activity via donating hydrogen mechanism, because the formed radical on Trolox can be stabilized by the delocalization within the aromatic ring. As mentioned above, sterically hindrance around the nitrogen atom of the DPPH radical inhibits all reactions, particularly the hydrogen transfer, which is necessary for the formation of a hydrogen-bonded complex. Complex molecules get in the way of each other more easily which blocks the access to DPPH radicals at low concentrations. Additionally, methanol, which is generally used as a solvent for the DPPH method, strongly binds H atoms and inhibits HAT processes. It may be concluded that DPPH$^{\bullet}$ radical might react with each antioxidant via different kinetics or might not react at all due to its stability. Furthermore, the reversibility of the reaction may lead to low readings of the antioxidant capacity of many antioxidants, consequently, the antioxidant capacity of many antioxidants is likely to be wrongly estimated.

3.1.3. FRAP Assay

The FRAP assay is a rapid and automated assay that measures the electron-donating ability of an antioxidant to reduce the ferric 2,4,6-tripyridyl-s-triazine complex $[Fe^{3+}\text{-}(TPTZ)_2]^{3+}$ to the intense, blue-colored ferrous complex $[Fe^{2+}\text{-}(TPTZ)_2]^{2+}$ under acidic condition (pH=3.6) [48]. Trolox equivalent (TE) is a unit of measurement used to express the antioxidant capacity of a substance relative to Trolox. All measurements for both Trolox and the sample should be done under the same conditions and concentrations [49]. The TE of ascorbic acid, RvD1, Analogue 1, and Analogue 2 were calculated based on the Trolox calibration curve. The TE values were obtained 242.53±46.16, 8.65±1.19, 12.71±2.51, and 14.12±2.14 µM at highest treated concentration (200 µM), respectively. Additionally, the relative percentage of reducing power were also calculated at the same concentrations and it was around 122.03%±22.81 for Ascorbic acid at 200 . However, this value for RvD1, Analogue 1, and Analogue 2 was much less, 4.12%±0.62, 6.17%±1.28, and 6.88%± 1.09, respectively (Figure 8). All data confirmed that the RvD1 analogues showed almost 2 times higher antioxidant activity compared to RvD1. To figure out why the analogues with potential antioxidant abilities have very little electron-donating ability compared to controls (ascorbic acid and Trolox), the redox condition mechanism should be considered. Redox conditions refer to media dominated by oxidants (electron acceptors), the substances that can oxidize other substances (cause them to lose electrons), or reductants (electron donors), the substances that can reduce other substances.

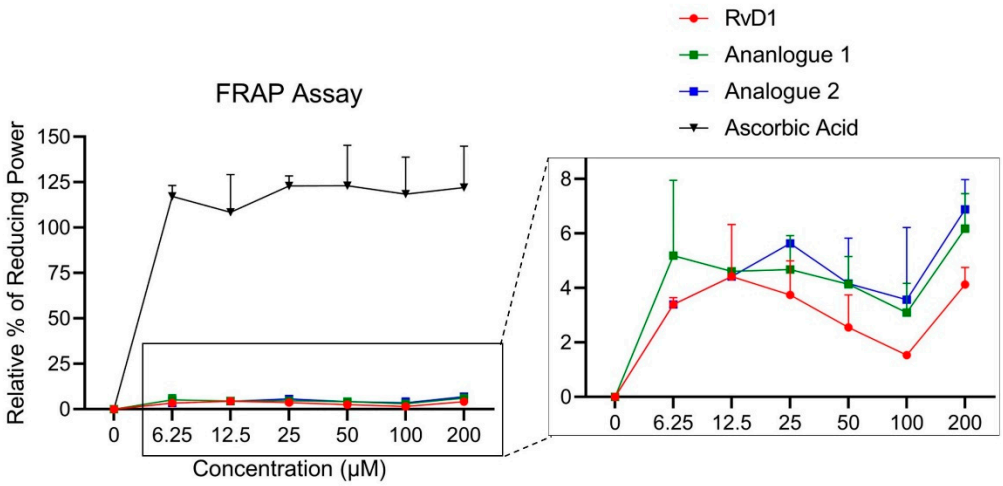

Figure 8. Relative percentage of reducing power of Ascorboc Acid, RvD1, Analogue 1, and Analogue 2 in compared to Trolox as a standard control using FRAP assay.

There are several possibilities that the RvD1 and its analogues are not able to donate electrons easily to the ferric ion (Fe^{3+}) and reduce it to a ferrous ion (Fe^{2+}). The first possible reason can be related to the standard reduction potentials (E° values) of the reactants which can vary depending on the

 doi:10.20944/preprints202402.1255.v1

specific reaction conditions and solvent properties. E° values represent the standard reduction potential under specific conditions of 25°C and 1 M concentration [50]. For example, the acidic condition of the FRAP reaction (pH=3.6) may cause the protonation of the antioxidant compounds and as a result, it prevents the transfer of electrons from the antioxidant to the ferric ion. In the case of Trolox, the specific E° value depends on the context of the reduction reaction. At neutral pH (7.4), the relevant E° value is around -0.48 V which indicates a stronger electron-donating tendency compared to the acidic condition (E° = -0.35 V). The E° value shifting at acidic pH is because of the protonation of the phenolic hydroxyl, affecting its electron-donating ability slightly. But in the case of ascorbic acid, the specific E° values at pH 7.4 and 4.5 are -0.28 V and -0.05 V, respectively. Although both Trolox and ascorbic acid are commonly used reference standards in the FRAP, Trolox generally has a more negative E°, indicating a stronger tendency to donate electrons and reduce ferric ions. This suggests it might show higher FRAP activity compared to ascorbic acid at neutral pH. On the other hand, from the mechanism point of view, Trolox donates a single electron via its phenolic hydroxyl group, but ascorbic acid can donate one or two electrons depending on pH and reaction conditions. Thus, the two-step electron-donating of ascorbic acid adds more complexity compared with Trolox. Regarding the RvD1 and its analogues, they showed much lower FRAP value compared to Trolox and ascorbic acid. It can be concluded that the E° value might be less negative to be able to reduce the Fe^{3+} with an E° value of +0.77V. To unravel the precise electron transfer processes involved in these antioxidants' activity, a comprehensive electrochemical studies is necessary to be done.

3.1.4. Hydroxyl Radical Scavenging (HRS)

This experiment was designed to investigate the antioxidant properties of RvD1 and analogues using $CuCl_2$ + H_2O_2-induced ROS generation in the acellular environment. Trolox was used as a positive control. As illustrated in Figure 9, RvD1, Analogue 1, Analogue 2, and Trolox reduced significantly the production of ROS in a time-dependent manner. After 8 h of incubation, the generation of ROS was reduced by 30, 50, 77, and 86 by Analogue 2, RvD1, Trolox, and Analogue 1, respectively, as compared to $CuCl_2$+H_2O_2 alone. These findings confirm the antioxidant activity of RvD1 and our synthetic analogues.

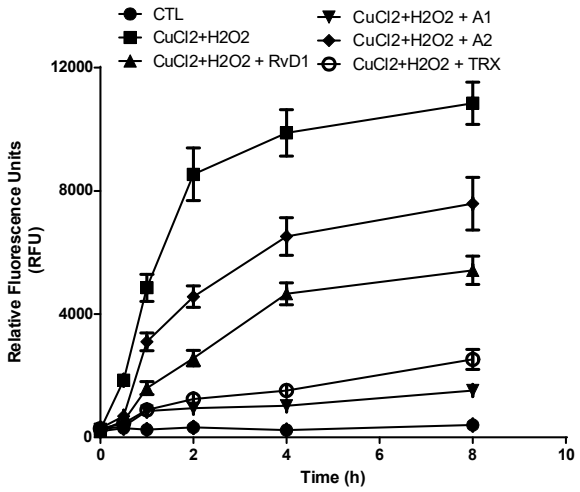

Figure 9. RvD1 and its analogues attenuate $CuCl_2$ + H_2O_2-induced ROS production. ROS were induced in a black 96-well plate by the addition of $CuCl_2$ (10 µM) to the H_2O_2 (100 µM) in the presence or absence of RvD1, Analogue 1 (A1), Analogue 2 (A2), and Trolox (TRX) at 10 µM. DCFH-DA probe was added at a concentration of 10 µM. The results are expressed as relative fluorescence units (RFU) (n=3).

3.2. Protection of Hyaluronic Acid against ROS

 doi:10.20944/preprints202402.1255.v1

Hyaluronic acid (HA) is a linear polysaccharide consisting of two alternating units, β-1,4-D-glucuronic acid and β-1,3-N-acetyl-D-glucosamine. HA, found in synovial fluid, acts as an elastoviscous component that creates a friction-free surface for joint movement. The molecular weight of HA is more variable and most commonly synthesized as a high-molecular-weight polymer in normal biological fluids and tissues, with an average molecular mass of approximately 1000–8000 kDa [51]. Studies have shown that HA concentration remains relatively stable with age or tends to decline between 28 and 40 years old and remains at a low level beyond that age. Its concentration in human synovial fluid ranges from 1.5 to 3.6 mg/mL. Hence, HA with an average molecular weight of 1500 kDa was dissolved in PBS buffer solution (pH 7.4, 150 mM) with a concentration of 2 mg/mL. Then, the HA solution was incubated with $CuCl_2$ + hydrogen peroxide (H_2O_2) without or in the presence of antioxidants (RvD1, Analogue 1, Analogue 2, and Trolox). To evaluate the radical scavenging capability of the antioxidants, the following studies were performed.

3.2.1. Agarose Gel Electrophoresis

Here, the capacity of RvD1 and analogues was investigated to block ROS-induced HA degradation. To do so, the polymer was treated with RvD1 and analogues and then after with $CuCl_2$ + H_2O_2 for 16 h. The degradation of HA was evaluated by gel agarose electrophoresis. As indicated in Figure 10, the addition of RvD1 and analogues protected $CuCl_2$ + H_2O_2-induced HA fragmentation and preserved its integrity of HA, as compared to the untreated HA.

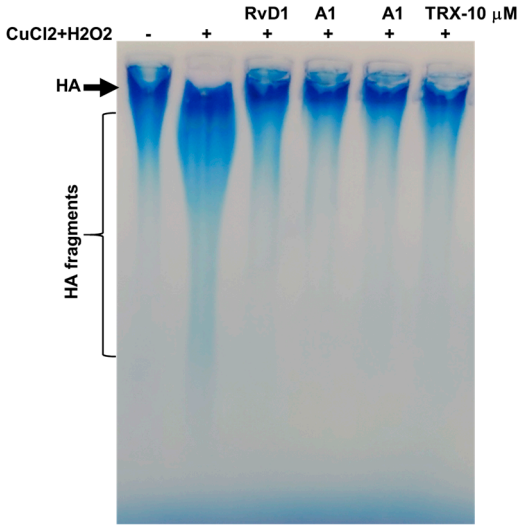

Figure 10. RvD1, Analogue 1 (A1), Analogue 2 (A2), and Trolox (TRX) inhibit $CuCl_2$ + H_2O_2-induced hyaluronic acid (HA) degradation. A solution of commercial HA (1 mg/mL, MW: 1000-2000 kDa) was exposed to 10 µM $CuCl_2$ and 100 µM H_2O_2 for 16 h in the presence or absence of RvD1, analogues or TRX at 10 µM. Samples were then loaded in agarose gel/1X TBE and then hyaluronic acid was revealed using a stain-all solution (n=3).

3.2.2. Gel Permeation Chromatography

Based on GPC results (Figure 11), the average molecular weight of HA was about 1,160,000 Da with a dispersity (Mw/Mn) of 1.103 and intrinsic viscosity of 13.5227. These values were changed significantly after the incubation of HA with hydrogen peroxide. The GPC chromatogram showed a symmetric broad peak with an average molecular weight of 217,211 Da, a dispersity value of 1.651, and an intrinsic viscosity of 4.7605. The degradation is because the hydroxyl radical can abstract hydrogen atoms at all ring C-H bonds except C-2 of N-acetyl hexosamine. The abstraction of hydrogen atoms generates carbon-center radicals which undergo a β-scission reaction resulting in the breakdown of the HA chains. ROS-mediated HA degradation occurs randomly and generates not only glycosidic linkage cleavage but also the possibility of other structural changes, including ring

 doi:10.20944/preprints202402.1255.v1

opening and the occurrence of different conformational characteristics. However, the RvD1 analogues as antioxidants scavenged the formed free radical and protected the HA from degradation. The GPC results showed that the average molecular weights of HA were almost the same as the control (free HA) which obtained 1,031.000, 1,043,000, and 1,026,000 Da for RvD1, Analogue 1, and Analogue 2, respectively. It can be concluded that the analogues have very good potential to protect HA from ROS degradation. All data obtained are summarized in Table 2 below which includes individual injection results.

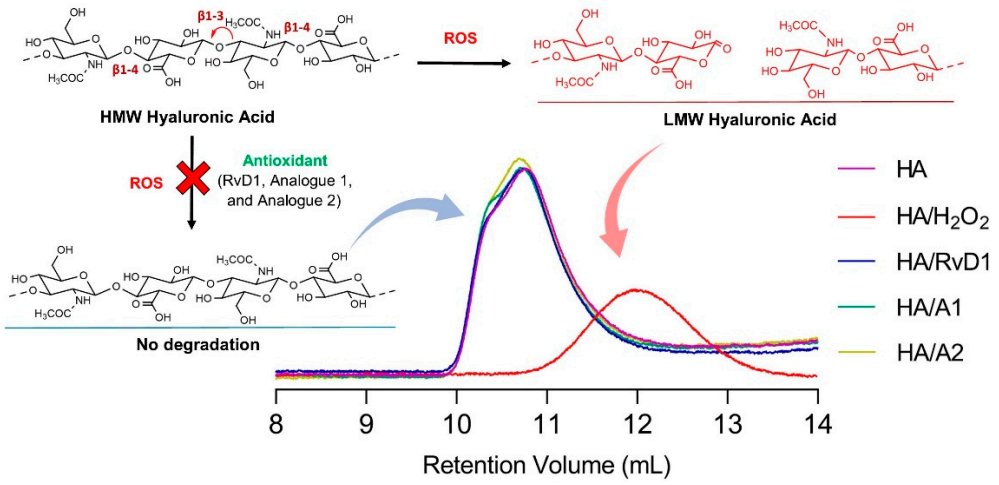

Figure 11. GPC/SEC Chromatogram. Molecular weight comparison of HA after incubation with $CuCl_2$+H_2O_2 without or in the presence of RvD1 and RvD1 analogues as radical scavengers.

Table 2. GPC/SEC data of hyaluronic acid degradation with H_2O_2 without or in the presence of RvD1 and its analogues (Triple detection GPC results of the samples were calculated using Refractive Index Increment (dn/dc) value of 0.158 mL/g for Hyaluronic Acid in water).

Sample	V_p[1] (mL)	M_w (Da)	M_n (Da)	M_w/M_n[2] (-)	IV[3] (mg/mL)
Hyaluronic Acid	10.76	1,160,000	1,052,000	1.103	13.5227
Hyaluronic Acid/H_2O_2	11.97	217,211	131,579	1.651	4.7605
Hyaluronic Acid/H_2O_2 + RvD1	10.75	1,113,000	1,031,000	1.079	13.9877
Hyaluronic Acid/H_2O_2 + A1	10.71	1,126,000	1,043,000	1.079	13.9109
Hyaluronic Acid/H_2O_2 + A2	10.70	1,112,000	1,026,000	1.084	13.6087

[1] Peak Retention Volume. [2] Polydispersity Index [3] Intrinsic Viscosity.

3.3. Computational Study

Experimental methods have been used to determine the total antioxidant activity of samples. However, for a comprehensive evaluation of the radical scavenging activity of samples, computational methods are required. In this study, two concepts were used to analyze the antioxidant activity of samples: hydrogen atom transfer (HAT, which is based on the electronic and thermal enthalpy), and single-electron transfer (which is based on the frontier orbital energies of neutral molecules).To attain this, some parameters were calculated, such as energy gap (ΔE), ionization potential (IP), bond dissociation enthalpy (BDE), hardness, softness, and electronegativity.

3.3.1. Geometry Optimization of samples

Geometry optimization is one of the most essential tasks in theoretical chemistry. It is a method to predict the three-dimensional arrangement of the atoms in a molecule employing the minimization of model energy. The molecular structures of all tested antioxidant samples are depicted in Figure 12

 doi:10.20944/preprints202402.1255.v1

(designed by ChemDarw software version 12.0.0). As shown, the molecules have several functional groups such as aromatic ring, hydroxyl (O-H), ester (O=C-OR), carboxylic acid (O=C-OH), and carbon-carbon conjugated double (C=C) bonds. Among all functional groups, there are only four main structural motifs that contribute to the antioxidant activity of small molecules. These functional motifs include hydroxyl groups (-OH), amino groups (-NH), thiol groups (-SH), and isoprenoid groups. In this study, all tested antioxidants are in common with hydroxyl functional groups, thus comparing the bond strength of their O-H can be a way to estimate their antioxidant potential. It was found that the weaker O-H bond shows a higher antioxidant potential. Therefore, to get more data about geometrical molecular structure and their bonds, the DFT method with B3LY/6-31G (d, p) function was performed for optimization and analysis of the antioxidant samples, including Trolox, Ascorbic acid, RvD1, Analogue 1, and Analogue 2 (Figure 13). The bond lengths obtained through the optimized molecular structure of different samples are useful data to explain the HAT.

Within the Trolox structure, there are two hydroxyls (O-H) bonds, and the bond lengths related to phenol (O7-H8) and carboxylic acid (O31-H32) are 0.9741 and 0.9821 Å, respectively. Based on the shorter the bond the stronger the bond, the hydroxyl bond in carboxylic acid should be weaker because of the higher bond length. Since the bond length difference is very low around >1%, the determination of the better hydrogen donating cannot be very precise. In the case of Ascorbic acid, its structure includes four hydroxyl groups and the shortest O-H bonds are O12-H13 and O8-H20 with a length equal to 0.9772 Å and 0.9791 Å. Whereas the longest value belongs to O9-H19 and O17-H18 with a length equal to 0.9797 Å. As a result, O9 and O17 in Ascorbic acid and O7 in Trolox can be supposed as the active sites for hydrogen donating. As seen in Table 3, the longer O-H bond lengths in RvD1, Analogue 1, and Analogue 2 were related to O56-H58, O60-H62, and O26-H27 with the bond lengths of 0.9996, 0.9821, and 0.9981 Å, respectively. Interestingly, the O-H bond related to the carboxylic bond showed a higher bond length compared to another hydroxyl bond in RvD1 and analogue 1. As the number and type of hydroxyl group in the tested molecules are different, comparing the hydrogen-donating properties of the molecules is not possible. Therefore, the average bond length of the hydroxyl group was calculated to show the order of the antioxidant capacity for Trolox, Ascorbic acid, RvD1, Analogue 1, and Analogue 2 (with average bond length of 0.9781, 0.9789, 0.9856, 0.9801, and 0.9856 Å, respectively).

Analogue 2 = RvD1 > Analogue 1 > Ascorbic acid > Trolox

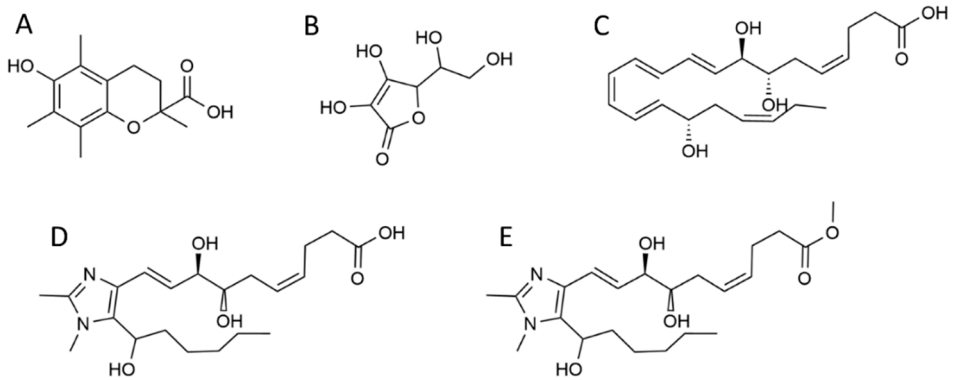

Figure 12. Molecular structure of Trolox (A), Ascorbic acid (B), RvD1 (C), Analogue 1 (D) and Analogue 2 (E).

 doi:10.20944/preprints202402.1255.v1

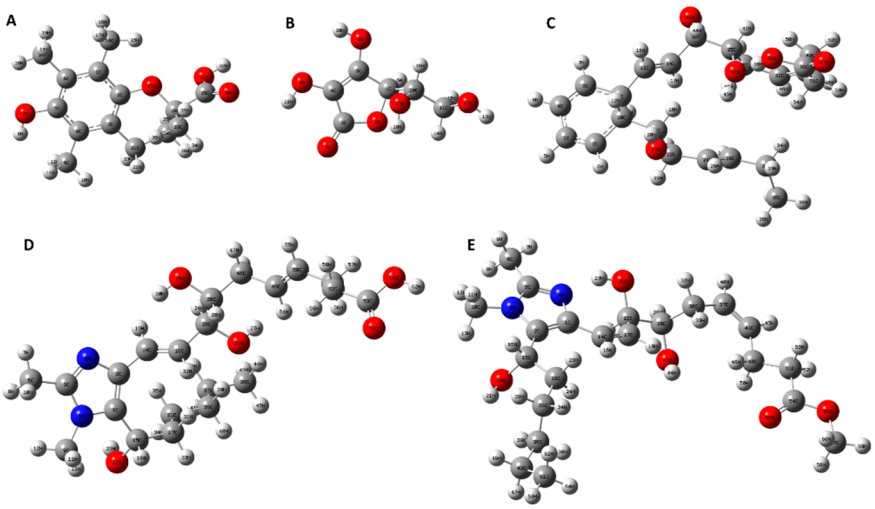

Figure 13. Geometrical molecular structure of Trolox (A), Ascorbic acid (B), RvD1 (C), Analogue 1 (D), and Analogue 2 (E) using Gaussian 09 - Ground states optimized at the B3LY/6-31G (d, p) function (all structures were also provided separately in the supporting information).

Table 3. Structural parameters of Trolox, Ascorbic acid, RvD1, Analogue 1, and Analogue 2: The bond length of the hydroxyl group (O-H).

Antioxidants	Bond	Bond Length (Å)*
Trolox	O7-H8	0.9741
	O31-H32	0.9821
Ascorbic acid	O8-H20	0.9791
	O9-H19	0.9797
	O12-H13	0.9772
	O17-H18	0.9797
RvD1	O19-H20	0.9786
	O42-H44	0.9821
	O43-H45	0.9824
	O56-H58	0.9996
Analogue 1	O22-H23	0.9795
	O25-H27	0.9780
	O29-H30	0.9808
	O60-H62	0.9821
Analogue 2	O20-H21	0.9795
	O26-H27	0.9981
	O43-H44	0.9793

* (1 Å = 10^{-10} m).

3.3.2. Bond Dissociation Enthalpy

Hydrogen Atom Transfer (HAT) is a crucial mechanism related to the antiradical activity of antioxidants. It is based on transferring hydrogen atoms with homolytic dissociation of O-H bond to free radicals. The antioxidant capacity of the HAT mechanism can be described by the Bond Dissociation Enthalpy (BDE) parameter.

$$BDE = H(ArO^{\bullet}) + H(H^{\bullet}) - H(ArOH) \quad (7)$$

Where H (ArOH) is the enthalpy of the neutral molecule, H ($ArO^{\bullet}$) is the enthalpy of the radical generated via H atom abstraction, and H ($H^{\bullet}$) is the enthalpy of H atom. The BDE values represent the energy necessary for cleaving the O-H bonds. The BDE values of all O-H bonds of samples are

 doi:10.20944/preprints202402.1255.v1

listed in Table 4. The antioxidant with the lowest BDE shows better antiradical properties. Table 4 shows clearly that the BDE value of O7-H8 of Trolox is the lowest in comparison with other hydroxyl groups in the gas phase. This means that the abstraction of the H atom from O7-H8 of Trolox is easier than other H atoms, which indicates that the radical created from this abstraction is more stable than other radicals. Moreover, among RvD1 and its analogues, the BDE value of the O22-H23 bond in the structure of Analogue 1 is the lowest, which indicates its higher antioxidant activity. According to the BDE values, the antioxidant activity of antioxidant samples decreases in the following order:

Trolox > Ascorbic acid > Analogue 1 > Analogue 2 > RvD1

All calculations of the neutral compounds and their radicals were calculated using Gaussian 09 software.

Table 4. O-H Bond Dissociation Enthalpy (BDE) of samples (kJ/mol).

Antioxidants	Bond	BDE
Trolox	O7-H8	280.9
	O31-H32	346.9
Ascorbic acid	O8-H20	290.3
	O9-H19	293.9
	O12-H13	383.6
	O17-H18	380.5
RvD1	O19-H20	471.4
	O42-H44	421.6
	O43-H45	385.4
	O56-H58	415.0
Analogue 1	O22-H23	375.4
	O25-H27	380.5
	O29-H30	401.9
	O60-H62	411.2
Analogue 2	O20-H21	386.2
	O26-H27	403.0
	O43-H44	378.5

3.3.3. Ionization Potential

Single electron transfer (SET) is another main mechanism of antioxidants, in which a single electron transfers from the antioxidant to the free radical. The antioxidant capacity of the SET mechanism can be described by the Ionization Potential (IP) parameter.

$$IP = H(ArOH^{\bullet+}) + H(e^-) - H(ArOH) \quad (6)$$

Where H (ArOH) is the enthalpy of the neutral molecule, H ($ArOH^{\bullet+}$) is the enthalpy of the radical cation, and H (e^-) is the enthalpy of a single electron. Ionization Potential (IP) shows the ease of electron removal from antioxidant samples. An antioxidant sample with a higher IP value shows a lower electron donation tendency, therefore, an electron is hardly removed from the HOMO orbital of the neutral form of the compound. On the other hand, a compound with a lower IP value has a higher electron transfer capacity. The IP values of samples are listed in Table 5. According to the data in Table 5, Trolox has the lowest Ionization potential, so an electron can be easily removed from the HOMO orbital of neutral Trolox. In contrast, Ascorbic acid has the highest IP, which indicates its low antioxidant activity via the SET mechanism in comparison to other samples. Concerning RvD1 and its analogues, Analogue 2 represents better electron donating properties. According to the IP values, the antioxidant activity of antioxidant samples decreases in the following order:

Trolox > Analogue 2 > Analogue 1 > RvD1 > Ascorbic acid

 doi:10.20944/preprints202402.1255.v1

Table 5. Ionization Potential (IP) of samples (kJ/mol).

Antioxidants	IP
Trolox	778.9
Ascorbic Acid	932.2
RvD1	875.3
Analogue 1	825.6
Analogue 2	806.1

3.3.4. Frontier Molecular Orbitals

Electronic properties of structures such as HOMO and LUMO energies and energy gaps (ΔE) of compounds can be evaluated using frontier molecular orbital theory. The HOMO (Highest Occupied Molecular Orbital) and LUMO (Lowest Unoccupied Molecular Orbital) are significant parameters that correlate with the antiradical activity of the samples. HOMO has electron donating ability; therefore, it is easy to remove electrons from this orbital. However, LUMO has electron accepting ability and it is easy for this orbital to accept electrons. To be more precise, in a compound with higher HOMO value, the donation of electrons is easier and as a result it may show better antioxidant activity. The electronic density distribution in the orbital permit's prediction of the most probable sites in a molecule that can be easily attacked by free radicals and other reactive agents.

The HOMO and LUMO energies and the ΔE (LUMO-HOMO) of all antioxidant samples with B3LYP/6-31 + G (d, p) basis set are shown in Figure 14. The energy of HOMO is related to the electron-donating ability of an antioxidant; however, the shape of HOMO shows the sites for free radical attack. As seen in Figure 14A, the HOMO of Trolox is localized over the whole molecule except for the carboxylic acid functional group. The results of HOMO and LUMO energies for Ascorbic acid (Figure 14B) showed that the HOMO is localized on O8-H20, O9-H19, and the lactone ring, while the LUMO is not localized on the lactone ring but is very close to it. In the case of RvD1 (Figure 14C) and its two analogues (Figure 14D,E), the HOMOs are localized on conjugated double bond and imidazolium ring, respectively. Theoretically, the energies of HOMO orbitals are a great indicator of the scavenging activity of samples, relating to their electron-donating ability. Thus, it can be concluded that these regions are the most probable sites for free radical attack. Based on all the above-mentioned results, it can be perceived that the HOMO energy of Trolox (-5.294 eV) is the highest and the lowest HOMO is related to Ascorbic acid (-6.554 eV), which means that the radical scavenging ability of Trolox should be much better than Ascorbic acid as controls. Additionally, the HOMO energy values for the RvD1, Analogue 1, and Analogue 2 are -6.045, -5.914, and -5.690 eV, respectively. Based on these results, Analogue 2 with the highest HOMO energy is more probable to donate electrons than RvD1 and Analogue 1. According to the HOMO energy values in all samples, it can be assumed that radical scavenging ability based on HOMO energy arrangement is as follows. This evidence confirms the IP results which are shown above.

Trolox > Analogue 2 > Analogue 1 > RvD1 > Ascorbic acid

 doi:10.20944/preprints202402.1255.v1

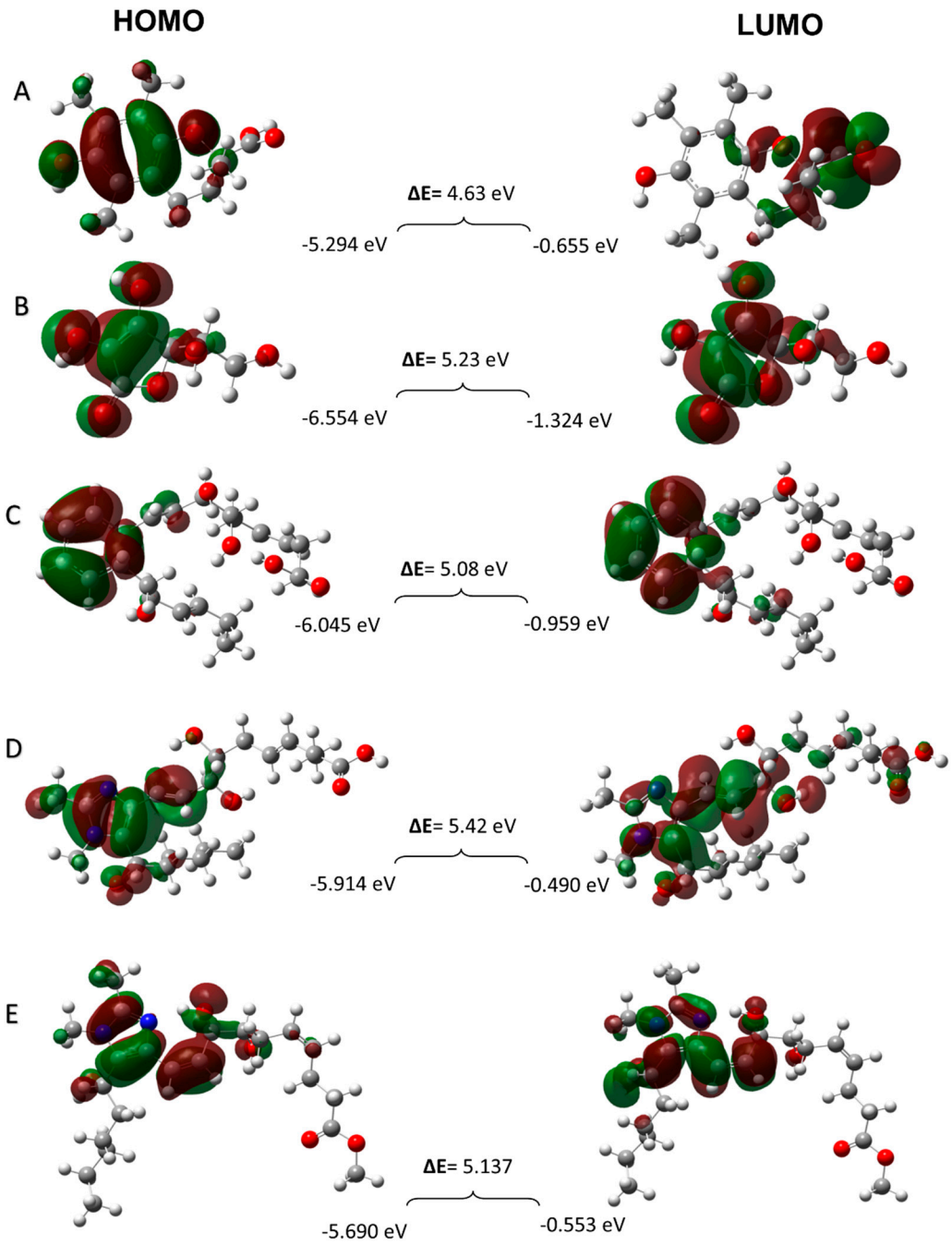

Figure 14. The energies and distributions of the HOMO and LUMO orbitals; Trolox (A), Ascorbic acid (B), RvD1 (C), Analogue 1 (D), and Analogue 2 (E).

3.3.5. Quantum chemical parameters

The chemical activity of compounds can be calculated by the frontier molecular orbitals energies (HOMO and LUMO). Hardness (η), softness (σ), electronegativity (χ), chemical potential (μ), and electrophilicity (ω) are the quantum chemical parameters to evaluate the chemical behavior of compounds. The polarizability of molecules is an important factor which is associated with the band gap energy. A molecule with high band gap energy shows less polarizability. Generally, soft molecules are more strongly polarizable than hard molecules, so the softness value shows the ability to transfer electrons. On the other hand, the hardness value is related to the resistance of the molecule to lose electrons. Therefore, the hard molecules have a high HOMO-LUMO gap (ΔE_{gap}) which tends to have high stability and low chemical reactivity with radicals. Overall, it may be said that the soft

 doi:10.20944/preprints202402.1255.v1

molecules have a low ΔE_{gap}, low stability, and high reactivity leading to higher antioxidant activity [52].

Electronegativity (χ) is the tendency of a molecule to attract electrons which is a factor to compare the antioxidant activity. According to the results, lower electronegativity is related to Trolox, which means that it has more ability to donate electrons rather than obtain them. Electrophilicity (ω) is the ability of a molecule to take up electrons from the surroundings and depicts the electron-accepting ability of species. Compounds with lower electrophilicity indexes are more likely to donate electrons and exhibit higher antioxidant activity. The lowest electrophilicity is related to Analogue 1 (the strongest antioxidant among under-studied samples), and the highest electrophilicity is related to Ascorbic acid (the weakest antioxidant among under-studied samples). The formula of all parameters is based on the Koopmans theorem's and is shown below. Tables 6 and 7 show the equation for quantum chemical parameters for the studied molecules and the calculated value for quantum chemical parameters, respectively.

Table 6. The equations for calculation of quantum chemical parameters of antioxidants.

Hardness (eV)	Softness (eV)	Electronegativity (eV)	Electrophilicity (eV)	Chemical Potential (eV)
$\eta = \frac{EL-EH}{2}$	$\sigma = \frac{1}{\eta}$	$\chi = \frac{-(EH+EL)}{2}$	$\omega = \frac{\chi^2}{2\eta}$	$\mu = -\chi$

Table 7. The calculation of quantum chemical parameters for antioxidants; hardness (η), softness (σ), electronegativity (χ), electrophilicity (ω), and chemical potential (μ).

Antioxidants	**E_{HOMO}**	**E_{LUMO}**	**η**	**σ**	**χ**	**ω**	**μ**
Trolox	-5.294	-0.655	2.31	0.432	2.974	1.914	-2.974
Ascorbic acid	-6.554	-1.324	2.61	0.383	3.938	2.970	-3.938
RvD1	-6.045	-0.959	2.54	0.393	3.500	2.411	-3.500
Analogue 1	-5.914	-0.490	2.71	0.369	3.201	1.890	-3.201
Analogue 2	-5.690	-0.553	2.56	0.390	3.121	1.902	-3.121

3.3.6. Molecular electrostatic potential (MEP)

The electrostatic potential map provides useful information related to the charge distribution of a molecule and information about the active sites of a molecule towards nucleophilic and electrophilic attack [53]. The MEP maps of antioxidant samples are shown in Figure 15. The electrostatic potential values of different sites are specified by different colors. The area with red color represents the most negative electrostatic potential (ESP, signifying electron-rich region for electrophilic attack), the blue color displays the most positive electrostatic potential (signifying electron deficient region for nucleophilic attack, such as radicals and charged molecules), and the green color illustrates the neutral electrostatic potential. Therefore, the negative ESP spots are significantly concentrated over oxygen atoms in all samples and nitrogen atoms in Analogues 1 and 2 (abundance of electrons in this region, active sites for electrophilic attack), and the positive ESP spots are mainly concentrated over some hydrogen atoms (absence of electrons in this region, active sites for nucleophilic attack) [54]. The most electronegative area (red region) is responsible for donating an electron and the most electropositive area (blue region) is responsible for donating proton.

 doi:10.20944/preprints202402.1255.v1

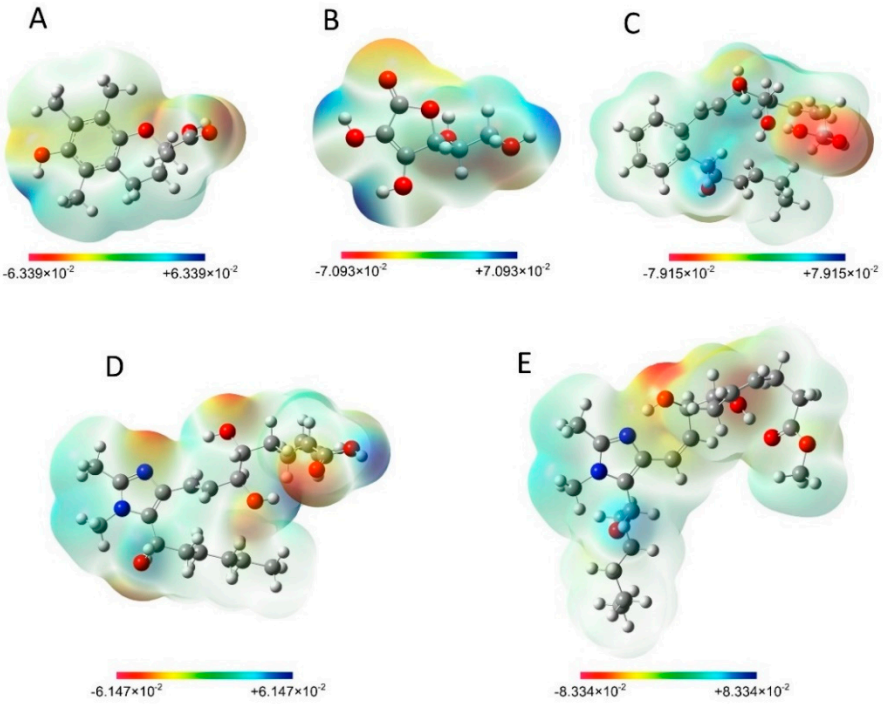

Figure 15. The molecular electrostatic potential surface (ESP) of Trolox (A), Ascorbic acid (B), RvD1 (C), Analogue 1 (D), and Analogue 2 (E).

3.3.7. Mulliken Charge Distribution

The Mulliken charge distribution of all samples is calculated on B3LYP at 6-31 G (d, p) level theory. Mulliken charge values for the atoms of all antioxidant samples are shown in Figure S9-13. In all samples, hydrogen atoms are positively charged, however, nitrogen and oxygen atoms acquire negative Mulliken atomic charge due to their electronegativity. Regarding carbon atoms, they are influenced by their substituents. Hence, all carbon atoms are negatively charged except for those which are boned with nitrogen and oxygen atoms. This is because electronegative atoms (N and O) pull out the partial charge from carbon atoms and make carbon atoms acquire a positive atomic charge.

5. Conclusions

Oxidative stress is closely linked to osteoarthritis progression and is a crucial target for therapy. Previous studies have reported that antioxidant treatment could reduce the degradation of the cartilage matrix and delay osteoarthritis progression. In the present study, new imidazolium RvD1 analogues as antioxidants with good potential for OA treatment were compared with commercially available RvD1. The *in vitro* chemical assay including ORAC, HRS, and FRAP assays showed that imidazolium RvD1 analogues have higher antioxidant capacities than commercially available RvD1. Interestingly, based on the ORAC assay the analogues demonstrated antioxidant capacity with 4 and 3 times more than Ascorbic acid and Trolox, respectively. Agarose gel electrophoresis results showed that the analogues have a good ability to protect HMW HA from degradation by ROS. The GPC analysis also confirmed the obtained results. To find the hydrogen and electron donating sites of the RvD1 analogues, a computational study using Gaussian 09 with DFT calculations and B3LYP/6-31 G (d, p) basis set was employed. The computational analysis data also validated that analogues have more hydrogen and electron-donating potential than RvD1. All findings proved that our newly designed imidazolium RvD1 analogues have good potential as antioxidant agents for OA treatment which encourages us to utilize them for further *in vivo* studies and antioxidant delivery systems in inflammatory disease treatment.

 doi:10.20944/preprints202402.1255.v1

Supplementary Materials: The following supporting information can be downloaded at the website of this paper posted on Preprints.org. Figure S1-5: Mulliken charge distribution for Trolox, RvD1, Analogue 1, and Analogue 2, respectively.

Author Contributions: Conceptualization, ZK, RM, JYS, DP, MB; methodology, ZK, CD, RM, JYS, MB.; software, ZK, MR.; formal analysis, ZK, CD, MR, RM, JYS, DP, MB.; writing—original draft preparation, ZK, MR, RM, JYS, MB.; writing—review and editing, ZK, CD, MR, JF, RM, JYS, DP, HF, MB.; supervision, DP, MB.; funding acquisition, HF, MB. All authors have read and agreed to the published version of the manuscript.

Funding: This work was supported by the Canadian Institutes of Health Research (CIHR) #MHP-185634 and by Axelys-Ministère d'Économie du Québec #AXE-0097 for BM and by The CIHR (PJT-1751110 and PJT-180297) for FH.

Institutional Review Board Statement: Not applicable.

Informed Consent Statement: Not applicable.

Data Availability Statement: Data are contained within the article and supplementary materials.

Conflicts of Interest: The authors declare no conflict of interest.

References

1. Di Nicola V: **Degenerative osteoarthritis a reversible chronic disease**. *Regenerative Therapy* 2020, **15**:149-160.
2. Rahimi M, Charmi G, Matyjaszewski K, Banquy X, Pietrasik J: **Recent developments in natural and synthetic polymeric drug delivery systems used for the treatment of osteoarthritis**. *Acta Biomaterialia* 2021, **123**:31-50.
3. McClurg O, Tinson R, Troeberg L: **Targeting Cartilage Degradation in Osteoarthritis**. In: *Pharmaceuticals.* vol. 14; 2021.
4. Mehana E-SE, Khafaga AF, El-Blehi SS: **The role of matrix metalloproteinases in osteoarthritis pathogenesis: An updated review**. *Life Sciences* 2019, **234**:116786.
5. Panahi Y, Alishiri GH, Parvin S, Sahebkar A: **Mitigation of Systemic Oxidative Stress by Curcuminoids in Osteoarthritis: Results of a Randomized Controlled Trial**. *Journal of Dietary Supplements* 2016, **13**(2):209-220.
6. Shi Q, Abusarah J, Zaouter C, Moldovan F, Fernandes JC, Fahmi H, Benderdour M: **New evidence implicating 4-hydroxynonenal in the pathogenesis of osteoarthritis in vivo**. *Arthritis Rheumatol* 2014, **66**(9):2461-2471.
7. Morquette B, Shi Q, Lavigne P, Ranger P, Fernandes JC, Benderdour M: **Production of lipid peroxidation products in osteoarthritic tissues: New evidence linking 4-hydroxynonenal to cartilage degradation**. *Arthritis & Rheumatism* 2006, **54**(1):271-281.
8. Kohen R, Nyska A: **Invited review: oxidation of biological systems: oxidative stress phenomena, antioxidants, redox reactions, and methods for their quantification**. *Toxicologic pathology* 2002, **30**(6):620-650.
9. Zhuang C, Wang Y, Zhang Y, Xu N: **Oxidative stress in osteoarthritis and antioxidant effect of polysaccharide from angelica sinensis**. *International Journal of Biological Macromolecules* 2018, **115**:281-286.
10. Tudorachi NB, Totu EE, Fifere A, Ardeleanu V, Mocanu V, Mircea C, Isildak I, Smilkov K, Cărăuşu EM: **The Implication of Reactive Oxygen Species and Antioxidants in Knee Osteoarthritis**. In: *Antioxidants.* vol. 10; 2021.
11. Henrotin Y, Mobasheri A: **Curcumin And Curcuminoids For The Treatment Of Osteoarthritis: Proof Of Concept**. *Journal of Tropical Medicinal Plants* 2009, **10**(2).
12. Berdiaki A, Neagu M, Spyridaki I, Kuskov A, Perez S, Nikitovic D: **Hyaluronan and Reactive Oxygen Species Signaling—Novel Cues from the Matrix?** In: *Antioxidants.* vol. 12; 2023.
13. Žádníková P, Šínová R, Pavlík V, Šimek M, Šafránková B, Hermannová M, Nešporová K, Velebný V: **The Degradation of Hyaluronan in the Skin**. In: *Biomolecules.* vol. 12; 2022.
14. Marinho A, Nunes C, Reis S: **Hyaluronic Acid: A Key Ingredient in the Therapy of Inflammation**. In: *Biomolecules.* vol. 11; 2021.
15. Schiller J, Volpi N, Hrabárová E, Šoltés L: **Hyaluronic acid: a natural biopolymer**. *Biopolymers: biomedical and environmental applications* 2011, **70**(1).

16. Soltés L, Kogan G, Stankovska M, Mendichi R, Rychlý J, Schiller J, Gemeiner P: **Degradation of high-molar-mass hyaluronan and characterization of fragments**. *Biomacromolecules* 2007, **8**(9):2697-2705.
17. Baron D, Baron H, Baerer C, Bodere C, Conrozier T: **Predictors for patient satisfaction of a single intra-articular injection of crosslinked hyaluronic acid combined with mannitol (HANOX-M-XL) in patients with temporomandibular joint osteoarthritis. Results of a prospective open-label pilot study (HAPPYMINI-ARTEMIS trial)**. *BMC Musculoskeletal Disorders* 2022, **23**(1):1-10.
18. Pegreffi F, Reginster J-Y, Bruyère O, Veronese N: **Comment on: The Effect of Intra-articular Hyaluronic Acid Injections and Payer Coverage on Total Knee Arthroplasty Procedures: Evidence From Large US Claims Database**. *Arthroplasty Today* 2023, **21**.
19. Bruyère O, Honvo G, Vidovic E, Cortet B: **Assessment of the Response Profile to Hyaluronic Acid Plus Sorbitol Injection in Patients with Knee Osteoarthritis: Post-Hoc Analysis of a 6-Month Randomized Controlled Trial**. *Biomolecules* 2021, **11**(10):1498.
20. Rinaudo M, Lardy B, Grange L, Conrozier T: **Effect of Mannitol on Hyaluronic Acid Stability in Two in Vitro Models of Oxidative Stress**. In: *Polymers*. vol. 6; 2014: 1948-1957.
21. Mendoza G, Alvarez AI, Pulido MM, Molina AJ, Merino G, Real R, Fernandes P, Prieto JG: **Inhibitory effects of different antioxidants on hyaluronan depolymerization**. *Carbohydr Res* 2007, **342**(1):96-102.
22. Mongkhon J-M, Thach M, Shi Q, Fernandes JC, Fahmi H, Benderdour M: **Sorbitol-modified hyaluronic acid reduces oxidative stress, apoptosis and mediators of inflammation and catabolism in human osteoarthritic chondrocytes**. *Inflammation Research* 2014, **63**:691-701.
23. Setti T, Arab MGL, Santos GS, Alkass N, Andrade MAP, Lana JFSD: **The protective role of glutathione in osteoarthritis**. *Journal of Clinical Orthopaedics and Trauma* 2021, **15**:145-151.
24. Henrotin Y, Kurz B: **Antioxidant to treat osteoarthritis: dream or reality?** *Current drug targets* 2007, **8**(2):347-357.
25. Suantawee T, Tantavisut S, Adisakwattana S, Tanavalee A, Yuktanandana P, Anomasiri W, Deepaisarnsakul B, Honsawek S: **Oxidative stress, vitamin e, and antioxidant capacity in knee osteoarthritis**. *Journal of clinical and diagnostic research: JCDR* 2013, **7**(9):1855.
26. Lee CH: **Role of specialized pro-resolving lipid mediators and their receptors in virus infection: a promising therapeutic strategy for SARS-CoV-2 cytokine storm**. *Archives of Pharmacal Research* 2021, **44**(1):84-98.
27. Yaribeygi H, Atkin SL, Simental-Mendía LE, Barreto GE, Sahebkar A: **Anti-inflammatory effects of resolvins in diabetic nephropathy: Mechanistic pathways**. *Journal of Cellular Physiology* 2019, **234**(9):14873-14882.
28. Molaei E, Molaei A, Hayes AW, Karimi G: **Resolvin D1, therapeutic target in acute respiratory distress syndrome**. *European Journal of Pharmacology* 2021, **911**:174527.
29. Benabdoune H, Rondon E-P, Shi Q, Fernandes J, Ranger P, Fahmi H, Benderdour M: **The role of resolvin D1 in the regulation of inflammatory and catabolic mediators in osteoarthritis**. *Inflammation Research* 2016, **65**(8):635-645.
30. Serhan CN, Petasis NA: **Resolvins and protectins in inflammation resolution**. *Chemical reviews* 2011, **111**(10):5922-5943.
31. Benabdoun HA, Kulbay M, Rondon EP, Vallieres F, Shi Q, Fernandes J, Fahmi H, Benderdour M: **In vitro and in vivo assessment of the proresolutive and antiresorptive actions of resolvin D1: relevance to arthritis**. *Arthritis Res Ther* 2019, **21**(1):72.
32. Norling LV, Headland SE, Dalli J, Arnardottir HH, Haworth O, Jones HR, Irimia D, Serhan CN, Perretti M: **Proresolving and cartilage-protective actions of resolvin D1 in inflammatory arthritis**. *JCI insight* 2016, **1**(5).
33. Dravid AA, Dhanabalan KM, Naskar S, Vashistha A, Agarwal S, Padhan B, Dewani M, Agarwal R: **Sustained release resolvin D1 liposomes are effective in the treatment of osteoarthritis in obese mice**. *Journal of Biomedical Materials Research Part A* 2023, **111**(6):765-777.
34. Inactivation E: **Resolvin D1 and Its Aspirin-triggered 17R Epimer**. *THE JOURNAL OF BIOLOGICAL CHEMISTRY* 2007, **282**(13):9323-9334.
35. Orr SK, Colas RA, Dalli J, Chiang N, Serhan CN: **Proresolving actions of a new resolvin D1 analog mimetic qualifies as an immunoresolvent**. *Am J Physiol Lung Cell Mol Physiol* 2015, **308**(9):L904-911.
36. Benderdour M, Fernandes J, Maltais R, Sanceau JY: **Resolvin Analogs Compounds, Methods and Used Thereof**. In: *WO2023137554A1*. vol. WO2023137554A1. Canada; 2023.

37. de Gaetano M, Butler E, Gahan K, Zanetti A, Marai M, Chen J, Cacace A, Hams E, Maingot C, McLoughlin A *et al*: **Asymmetric synthesis and biological evaluation of imidazole- and oxazole-containing synthetic lipoxin A4 mimetics (sLXms)**. *European Journal of Medicinal Chemistry* 2019, **162**:80-108.
38. Huang D, Ou B, Hampsch-Woodill M, Flanagan JA, Prior RL: **High-Throughput Assay of Oxygen Radical Absorbance Capacity (ORAC) Using a Multichannel Liquid Handling System Coupled with a Microplate Fluorescence Reader in 96-Well Format**. *Journal of Agricultural and Food Chemistry* 2002, **50**(16):4437-4444.
39. Goldschmidt S, Renn K: **Zweiwertiger Stickstoff: Über das α, α-Diphenyl-β-trinitrophenyl-hydrazyl.(IV. Mitteilung über Amin-Oxydation)**. *Berichte der deutschen chemischen Gesellschaft (A and B Series)* 1922, **55**(3):628-643.
40. Blois MS: **Antioxidant Determinations by the Use of a Stable Free Radical**. *Nature* 1958, **181**(4617):1199-1200.
41. Benzie IFF, Strain JJ: **The Ferric Reducing Ability of Plasma (FRAP) as a Measure of "Antioxidant Power": The FRAP Assay**. *Analytical Biochemistry* 1996, **239**(1):70-76.
42. Govindappa CM, Sadananda TS, Chandrappa CP: **Phytochemical Analysis of Loranthus micranthus Extracts and Their in Vitro Antioxidant and Antibacterial Activities**. *Journal of Biologically Active Products from Nature* 2014, **4**(4):303-315.
43. Chen H, Qin J, Hu Y: **Efficient Degradation of High-Molecular-Weight Hyaluronic Acid by a Combination of Ultrasound, Hydrogen Peroxide, and Copper Ion**. *Molecules* 2019, **24**(3).
44. Yogesh K, Jha SN, Ahmad T: **Antioxidant potential of aqueous extract of some food grain powder in meat model system**. *Journal of Food Science and Technology* 2014, **51**(11):3446-3451.
45. Foti MC: **Use and Abuse of the DPPH• Radical**. *Journal of Agricultural and Food Chemistry* 2015, **63**(40):8765-8776.
46. Munteanu IG, Apetrei C: **Analytical Methods Used in Determining Antioxidant Activity: A Review**. In: *International Journal of Molecular Sciences*. vol. 22; 2021.
47. Gulcin İ, Alwasel SH: **DPPH radical scavenging assay**. *Processes* 2023, **11**(8):2248.
48. Lang Y, Gao N, Zang Z, Meng X, Lin Y, Yang S, Yang Y, Jin Z, Li B: **Classification and antioxidant assays of polyphenols: a review**. *Journal of Future Foods* 2024, **4**(3):193-204.
49. Gliszczyńska-Świgło A: **Antioxidant activity of water soluble vitamins in the TEAC (trolox equivalent antioxidant capacity) and the FRAP (ferric reducing antioxidant power) assays**. *Food chemistry* 2006, **96**(1):131-136.
50. Baranowska M, Suliborska K, Chrzanowski W, Kusznierewicz B, Namieśnik J, Bartoszek A: **The relationship between standard reduction potentials of catechins and biological activities involved in redox control**. *Redox Biology* 2018, **17**:355-366.
51. Cowman MK, Lee H-G, Schwertfeger KL, McCarthy JB, Turley EA: **The Content and Size of Hyaluronan in Biological Fluids and Tissues**. *Frontiers in Immunology* 2015, **6**.
52. Nasidi II, Kaygili O, Majid A, Bulut N, Alkhedher M, ElDin SM: **Halogen Doping to Control the Band Gap of Ascorbic Acid: A Theoretical Study**. *ACS omega* 2022, **7**(48):44390-44397.
53. Tabrizi L, Nguyen TLA, Dao DQ: **Experimental and theoretical investigation of cyclometalated phenylpyridine iridium(iii) complex based on flavonol and ibuprofen ligands as potent antioxidant**. *RSC Advances* 2019, **9**(30):17220-17237.
54. Farrokhnia M: **Density Functional Theory Studies on the Antioxidant Mechanism and Electronic Properties of Some Bioactive Marine Meroterpenoids: Sargahydroquionic Acid and Sargachromanol**. *ACS Omega* 2020, **5**(32):20382-20390.